The Impact of the Land Surface Physics in the Operational NCEP Eta Model on Simulating the Diurnal Cycle: Evaluation and Testing Using Oklahoma Mesonet Data

CURTIS H. MARSHALL* AND KENNETH C. CRAWFORD

Oklahoma Climatological Survey, University of Oklahoma, Norman, Oklahoma

KENNETH E. MITCHELL

NOAA/NWS/NCEP/Environmental Modeling Center, Washington, D.C.

DAVID J. STENSRUD

NOAA/National Severe Storms Laboratory, Norman, Oklahoma

(Manuscript received 24 September 2002, in final form 3 March 2003)

ABSTRACT

On 31 January 1996, the National Centers for Environmental Prediction/Environmental Modeling Center (NCEP/EMC) implemented a state-of-the-art land surface parameterization in the operational Eta Model. The purpose of this study is to evaluate and test its performance and demonstrate its impacts on the diurnal cycle of the modeled planetary boundary layer (PBL). Operational Eta Model output from summer 1997 are evaluated against the unique observations of near-surface and subsurface fields provided by the Oklahoma Mesonet. The evaluation is partially extended to July 1998 to examine the effects of significant changes that were made to the operational model configuration during the intervening time.

Results indicate a severe positive bias in top-layer soil moisture, which was significantly reduced in 1998 by a change in the initialization technique. Net radiation was overestimated, largely because of a positive bias in the downward shortwave component. Also, the ground heat flux was severely underestimated. Given energy balance constraints, the combination of these two factors resulted in too much available energy for the turbulent fluxes of sensible and latent heat. Comparison of model and observed vertical thermodynamic profiles demonstrates that these errors had a marked impact on the model PBL throughout its entire depth. Evidence also is presented that suggests a systematic underestimation of the downward entrainment of relatively warmer, drier air at the top of the PBL during daylight hours.

Analyses of the monthly mean bias of 2-m temperature and specific humidity revealed a cool, moist bias over western Oklahoma, and a warm, dry bias over the eastern portion of the state. A very sharp transition existed across central Oklahoma between these two regimes. The sharp spatial gradient in both the air temperature and humidity bias fields is strikingly correlated with a sharp west–east gradient in the model vegetation greenness database. This result suggests too much (too little) latent heat flux over less (more) vegetated areas of the model domain.

A series of sensitivity tests are presented that were designed to explore the reasons for the documented error in the simulated surface fluxes. These tests have been used as supporting evidence for changes in the operational model. Specifically, an alternative specification for the soil thermal conductivity yields a more realistic ground heat flux. Also, the alternative thermal conductivity, when combined with a slight adjustment to the thermal roughness length, yields much better internal consistency among the simulated skin temperature and surface fluxes, and better agreement with observations.

1. Introduction

Recognizing the importance of adequately representing the effects of land surface processes in numerical weather prediction models, the National Centers for Environmental Prediction/Environmental Modeling Center (NCEP/EMC) implemented a state-of-the-art land surface parameterization in the operational Eta Model on 31 January 1996 (Chen et al. 1996, 1997; Betts et al. 1997; Ek et al. 2003). Implementation of the land surface parameterization was also accompanied by changes to the atmospheric surface-layer treatment in the planetary boundary layer (PBL) scheme. Following the original implementation of the land surface treatment, a number of verification and testing studies, including this work, provided the scientific basis for a series of chang-

* Current affiliation: Department of Atmospheric Science, Colorado State University, Fort Collins, Colorado.

Corresponding author address: Curtis H. Marshall, Dept. of Atmospheric Science, Colorado State University, Fort Collins, CO 80523.
E-mail: cmarshall@atmos.colostate.edu

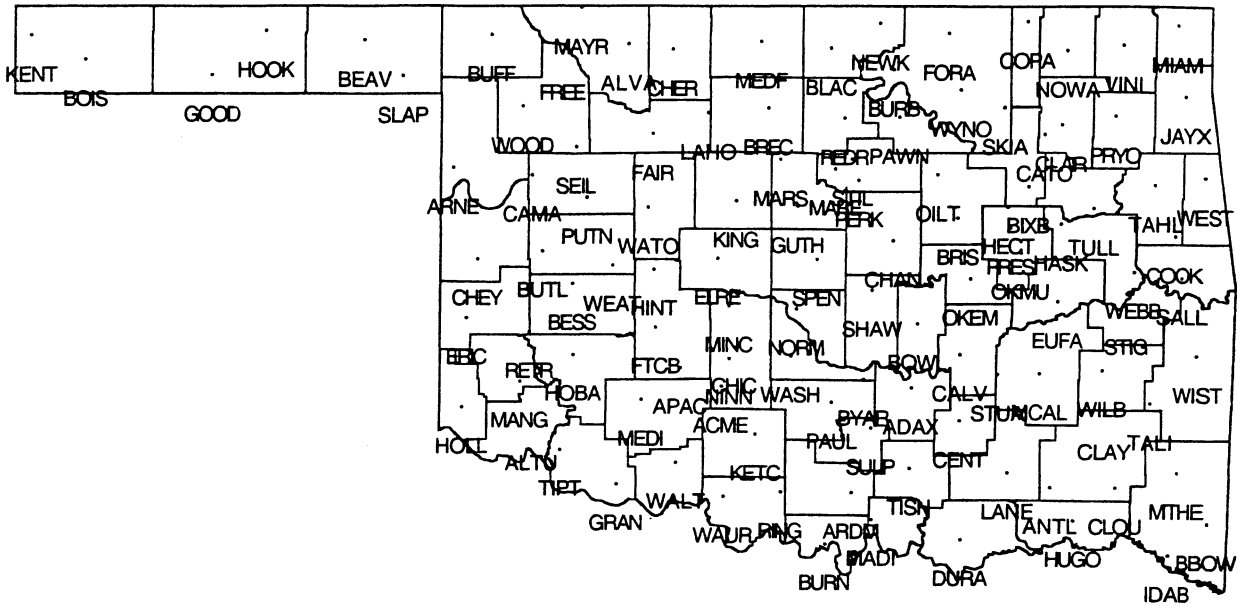

FIG. 1. Locations and four-letter identifiers for each of the 115 stations of the OK Mesonet. The average station spacing is approximately 32 km.

es and upgrades to the operational model physics. These upgrades have supported the goal of improving the simulated fluxes of heat and water vapor at the land surface—processes that are critical in simulating the diurnal evolution of the PBL (Pielke et al. 1991). The purpose of this paper is to present an evaluation of the versions of the model physics that were operational during the warm seasons of 1997 and 1998, with an emphasis on demonstrating their practical impact on the model-simulated diurnal cycle.

Previous studies, such as Betts et al. (1997) and Chen et al. (1996, 1997) have evaluated and tested the land surface and surface-layer schemes of the Eta Model by comparing observed data at a single site to model time series at a single grid point, with both uncoupled and coupled model configurations. In the uncoupled tests, the land surface parameterization was forced with observed atmospheric data, while in the coupled mode the scheme was fully interactive with the atmospheric Eta Model. This study is unique in that fully three-dimensional fields of operational coupled model output (in addition to single-point time series), including soil state variables and surface energy fluxes, were examined over a spatial domain characterized by widely varying climate and land use regimes for extended periods of time, using the unique observations provided by the Oklahoma Mesonet (Brock et al. 1995).

The Oklahoma Mesonet is a high-resolution hydrometeorological observing network covering the state of Oklahoma, which measures near-surface and subsurface fields at a spatial resolution ideal for verification of mesoscale models (Fig. 1). The domain spans a wide contrast of land surface and climate regimes. The far west, a high plains grassland environment, receives less than 20 in. of annual precipitation, while the eastern section of the network domain is a deciduous forest with an annual rainfall exceeding 45 in. (Johnson and Duchon 1995). Recently, the network was upgraded to include a comprehensive soil moisture observing system. Along with standard meteorological variables, simulated soil states from the operational output are evaluated against these unique observations. Furthermore, an additional suite of instruments was located at one site to provide estimates of surface energy fluxes.

2. Model description

The Eta Model (Black 1994), the primary numerical prediction system for providing regional and mesoscale forecast guidance for and from the National Weather Service (NWS), is named after its step-mountain vertical coordinate (η) defined by Mesinger (1984). The operational model is embedded in the larger framework of the Eta Data Assimilation System (EDAS; Rogers et al. 1996). The EDAS functions as a continuous series of 3-h ''miniforecasts'' (Fig. 2). Each miniforecast provides the initial conditions (background field) for a subsequent objective analysis. The new analysis provides the initial condition for the next 3-h forecast. This scenario is repeated ad infinitum. Every 6 h, a ''free forecast'' (which was produced out to 48 h for the operational configuration at the time of this study) is produced using the latest analysis as its initial state. In theory, a free forecast could be produced from every analysis. However, practical constraints in the operational computing environment limit this capability.

A key point to understand is that the EDAS is now continuously cycling as a self-contained system. The

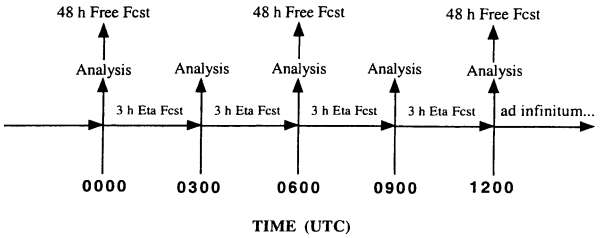

FIG. 2. Schematic of the operational configuration of the EDAS analysis cycle and Eta Model free forecasts during the period of this study after Rogers et al. (1996).

background field for each objective analysis is derived solely from the previous miniforecast. Prior to 9 June 1998 the EDAS cycling was divided into 12-h segments, and the background for the first analysis in a given segment was derived from the NCEP Global Model Data Assimilation System (GDAS; Kanamitsu et al. 1991). The new self-contained EDAS cycling procedure has important implications for land surface state variables in the Eta Model (namely, soil moisture and soil temperature). Because routine observations of subsurface parameters do not exist, no assimilation of soil temperature and moisture data is performed in the EDAS during the analysis step. Thus, these fields evolve continuously only in response to external coupled model forcing on the land surface physics (e.g., coupled model rainfall and radiation). In comparison, three-dimensional atmospheric fields (e.g., mass and momentum) are adjusted to observational data every 3 h via the mathematical techniques of data assimilation.

a. Land surface parameterization scheme

After extensive evaluation and testing of several candidate land surface treatments, the Eta Model scheme emerged from extensions to the Oregon State University (OSU) model of Pan and Mahrt (1987). The original OSU model consists of the diurnally dependent Penman potential evaporation formulation of Mahrt and Ek (1984), the soil model of Mahrt and Pan (1984), and the primitive canopy model of Pan and Mahrt (1987). Extensions include the canopy resistance model following Noilhan and Planton (1989) and Jacquemin and Noilhan (1990), and the surface runoff formulation described by Schaake et al. (1996). Recently, improved snowpack and frozen soil physics were added to the operational configuration. In the operational environment, refinements and additions to model physics are an ongoing process. In this section, attention will be given to the physics present in the model versions that were operational for the time period covered by this study. Ek et al. (2003) provide a comprehensive review of the current operational configuration, including recent changes and performance. The following discussion provides a brief description of the model physics, with an emphasis on those relationships that are important to interpretation of the results presented in this paper.

The land surface physics are driven by atmospheric inputs in a fully coupled fashion. Model fields of surface radiation, precipitation, and near-surface winds and thermodynamic quantities provide the external forcing for the land surface. The soil module during the 1997 period of this study consisted of two layers: a thin top layer of 10 cm, and a deep root zone of 190 cm. Even though the parameterization could accommodate more layers, this configuration was chosen to be consistent with the NCEP GDAS, from which soil moisture and soil temperature were initialized during that time. In companion to changes in atmospheric horizontal and vertical resolution on 9 February 1998, the number of soil layers was increased to four. The layer thicknesses (from top to bottom) are 10, 30, 60, and 100 cm. The land surface parameterization provides the atmospheric portion of the Eta Model with surface latent heat flux, and a ground surface temperature, from which surface sensible heat flux and upward longwave radiation are diagnosed.

The prognostic variable for soil moisture, the volumetric soil water (θ), is defined as the fraction of the volume of soil medium occupied by liquid water. The soil medium consists of solid soil particles, water, and air space (the most recent version includes soil ice). The prognostic equation for the volumetric soil water content, Richard's equation (Hanks and Ashcroft 1986), is expressed in terms of the soil water diffusivity (D) and hydraulic conductivity (K). Both K and D are functions of soil type and θ. The soil-dependent empirical functions of Cosby et al. (1984) are used to diagnose their values. The soil type is specified based on the 1°, nine-class database of Zobler (1986). The sources and sinks for soil water are precipitation and evaporation, where the difference between the precipitation not intercepted by the canopy and the surface runoff represents the infiltration of water into the soil at the upper boundary. The surface runoff approach outlined by Schaake et al. (1996) statistically accounts for subgrid-scale effects by allowing gridded runoff to occur without requiring complete saturation of the soil column.

Evaporation from the land surface (E) is the sum of three components:

$$E = E_{\text{dir}} + E_t + E_c, \tag{1}$$

where E_{dir}, E_t, and E_c are direct (bare soil) evaporation, canopy transpiration, and evaporation of canopy-intercepted rainfall, respectively. Outside periods of model rainfall, the first two terms in (1) dominate the total evapotranspiration. In this study, data collected during periods of model and/or observed rainfall are excluded from the analysis. The separate components of the total evapotranspiration are represented mathematically by their resistance effects on the potential evaporation (E_p), which incorporates energy balance constraints to impose a limiting value of E.

A hallmark of the land surface treatment is the use of a satellite-derived database of spatially and temporally varying vegetation greenness. The green vegeta-

tion fraction (σ_f) is defined as the model grid-cell fraction wherein midday downward solar radiation is intercepted by the photosynthetically active green canopy. The Eta Model currently utilizes a 0.144° monthly database based upon a 5-yr satellite climatology developed at the National Environmental Satellite, Data, and Information Service (NESDIS) (Gutman and Ignatov 1998). The σ_f values are derived from the normalized difference vegetation index (NDVI), the latter obtained from the National Oceanic and Atmospheric Administration (NOAA) Advanced Very High Resolution Radiometer (AVHRR) satellite. This parameter acts as a fundamental weighting factor between bare soil evaporation and canopy transpiration. Thus, over areas of relatively high (low) greenness fraction, the total evapotranspiration in (1) is dominated by E_t (E_{dir}).

Proper representation of canopy resistance in a land surface scheme is of first-order importance in simulating the evapotranspiration. After rainfall (when soil moisture is high), the canopy resistance acts to constrain the evaporation rate below the potential value. Conversely, during dry periods, the canopy can effectively tap deeper root zone soil moisture and sustain the model evaporation rate (Kim and Verma 1990). The canopy resistance formulation is expressed in terms of the minimum stomatal resistance (R_{cmin}), which is a measure of the degree to which plant stomata expend water vapor during photosynthesis. Its value is specified based on the vegetation type. The Eta Model utilizes the 1° database of 12 vegetation classes developed at the University of Maryland for the Simple Biosphere Model (Xue et al. 1996). The overall canopy resistance is a modification of R_{cmin} that incorporates the stress effects of solar radiation, vapor pressure deficit, air temperature, and soil moisture availability.

The prognostic temperature in the four soil layers is determined by the ground heat flux, which is represented with a classic heat diffusion equation expressed in terms of the volumetric heat capacity [$C(\theta)$] and soil thermal conductivity [$K_t(\theta)$]. A numerical solution of the diffusion equation requires upper- and lower-boundary conditions. The soil temperature at the lower boundary (applied at 3 m during the period of this study) is taken as the annual mean air temperature at the model grid point in question. The ground surface temperature (T_{skin}), used to diagnose the sensible heat flux and the upward longwave component of the net radiation, is determined from the surface energy balance equation:

$$\text{RNET} = \text{FXSH} + \text{FXLH} + \text{FXGH}, \qquad (2)$$

which shows that the net radiation (RNET) is equal to the sum of the sensible heat flux (FXSH), the latent heat flux (FXLH), and the ground heat flux (FXGH). The expanded form of the four terms in (2) is expressed in terms of T_{skin}. Thus, an iterative technique is required for its solution at a given model time step. The energy balance equation is the basis of the land surface scheme. Indeed, the scheme can be mathematically reduced to (2).

b. Atmospheric surface layer

The atmospheric surface layer is traditionally defined as the constant flux layer—that section of the PBL within a few tens of meters of the surface of the earth wherein the turbulent fluxes are assumed to be nearly constant with height (Sorbjan 1989). In the Eta Model, the first model layer (between the ground surface and the first Eta surface) is defined to be the surface layer. Over the domain of the Oklahoma Mesonet, the first Eta surface (as present in the vertical grid configuration operational during the time period covered by this study) is typically between 50 and 70 m above ground level. The purpose of the surface-layer physics is to provide the primary means of coupling the atmosphere to the land surface through the specification of the aerodynamic resistance to the surface fluxes (in comparison to the land surface physics, which provide resistance to the fluxes via, e.g., the stomatal resistance). Additionally, the parameterization is used to diagnose surface-layer vertical profiles and shelter-level estimates of wind, temperature, and humidity. Janjić (1994) provides details on the Mellor–Yamada level-2.5 turbulence closure scheme (Mellor and Yamada 1974), which is used to parameterize vertical turbulent exchange above the surface layer.

The detail in the surface-layer scheme lies in the parameterization of the surface exchange coefficient (i.e., the inverse of the aerodynamic resistance, C_h), which is expressed using Monin–Obukhov similarity theory (Monin and Obukhov 1954). The basis of similarity theory is the use of characteristic (similar) relationships between fluxes and profiles in the surface layer. The empirical stability functions and the Monin–Obukhov length scale (not shown) mathematically express the similarity by scaling the characteristic flux-profile relationships with dimensionless parameters that account for important factors such as surface roughness and surface-layer static stability.

The changes that were made to the surface-layer scheme on 31 January 1996 involved the replacement of the empirical stability functions of Łobocki (1993) with the Paulson (1970) formulations, and the addition of a new treatment of the roughness length for heat. In testing three different surface-layer parameterization schemes for the Eta Model, Chen et al. (1997) found no significant differences in the surface fluxes regardless of the choice of empirical stability functions, provided that the same representation of the roughness length for heat was employed. The sensitivity to the empirical treatment of the thermal roughness length is examined in detail in section 6.

3. Datasets and analysis methodology

The time of year chosen for study, May–July, was chosen because it is the heart of the warm season in

Oklahoma, when vegetation is actively transpiring and the diurnal cycle of PBL growth and decay is most vigorous. Furthermore, this time of year is characterized by a relative lack of synoptic–dynamic forcing (especially later in the period), allowing the signal from land surface processes to dominate the diurnal cycle of PBL thermodynamic fields.

A combination of gridded model fields and hourly time series at one grid point are examined over the May–July 1997 period, with particular emphasis on July. The analysis is extended to July 1998 for a subset of these fields, to revisit the performance of the model after the operational implementation of continuous self-cycling in the EDAS (9 June 1998) and the increase in the number of soil layers from two to four (9 February 1998). While most of the results presented in this paper are comparisons of July 1997 to July 1998 model performance, limited results from the other two months in 1997 are presented. Additionally, one highly representative 48-h model cycle is chosen from both July periods to illustrate key points, and a series of sensitivity analyses are presented using the 1998 case as the experimental control.

a. Gridded model fields

Gridded data from each 1200 UTC operational Eta Model run are verified at 6-h intervals with mesonet observations. Because each forecast cycle extended out to 48 h, there are nine separate realizations from each run to verify. The differences between model and observed values are used to produce monthly mean bias fields for each of the nine realization times. In order to produce these gridded difference fields, observational data were interpolated to the model grid using a three-pass Barnes objective analysis scheme. These fields provide critical insight into the spatial variability of model performance across Oklahoma during a 48-h model cycle, giving more information than a single-point time series verification otherwise could. The gridded fields verified include 2-m air temperature, 2-m specific humidity, surface downward solar radiation, 5-cm soil temperature, and 5-cm soil moisture. Unfortunately, verification of deep-layer soil moisture and temperature was not permitted because of differences between model-predicted and measurement depths. The soil-layer configuration throughout this study included a 10-cm top layer, with its predictive level of 5 cm corresponding to one of the depths of temperature and moisture measurements within the mesonet. In section 3c, we discuss the error and uncertainty associated with soil moisture measurements in more detail.

b. Diurnal time series

The verification of gridded data across the mesonet domain provides insight into model performance over the large, geographically complex, and climatologically diverse region covered by the network. However, the primary purpose of this study is to demonstrate how model inadequacies in the land surface physics and simulation of land surface state variables impact the diurnal behavior of the PBL through the influence of the surface fluxes. Thus, monthly mean diurnal time series of model and observed surface fluxes, subsurface fields, and standard meteorological parameters valid for the location of the Norman, Oklahoma, mesonet site (NORM) are also analyzed in this study. NORM is a location at which diurnal time series of Eta Model near-surface and subsurface fields are archived by EMC at hourly resolution (in contrast to gridded data, which are available only every 6 h). In order to ascertain the greatest level of accuracy for comparison with the point measurement time series, the model hourly output were interpolated from the four model grid points surrounding the precise location of NORM. Because we are concerned primarily with the performance of the model physics under synoptically quiescent conditions, in which the signal from the land surface dominates the diurnal cycle of PBL growth and decay, cloudy days and days with precipitation at NORM (in both model and observations) have been eliminated from the monthly composite time series.

In companion to the diurnal time series at NORM, selected model and observed vertical thermodynamic profiles are also examined to investigate the impacts of the simulated surface fluxes (and their associated errors) on the structure of the model PBL. The observational profiles were provided from the nearby (about 1 km) rawinsonde site at the Norman, Oklahoma, NWS forecast office.

c. Mesonet data

1) INTRODUCTION

The Oklahoma Mesonet has been archiving routine observations of standard meteorological observations since 1994. Brock et al. (1995) provide a comprehensive discussion of instrument specifications and operational procedures, including error statistics for the instrument platforms used for measurement of standard meteorological parameters. Beginning in the mid-1990s, new observations were added to the mesonet infrastructure to facilitate the measurement of various hydrometeorological fields required to quantify land–atmosphere interaction. Soil temperature observations are available at 5 and 10 cm under both bare soil and native vegetation. In spring 1996, soil moisture sensors were added at depths of 5, 25, 60, and 75 cm. Data from a variety of additional instrument platforms that have been periodically located at NORM for various field campaigns and special observing periods were taken advantage of for this study. Net radiation was measured during summer 1997 with a broadband net radiometer. However, during July 1998 measurements of all four individual components of the total net radiation (up- and downward

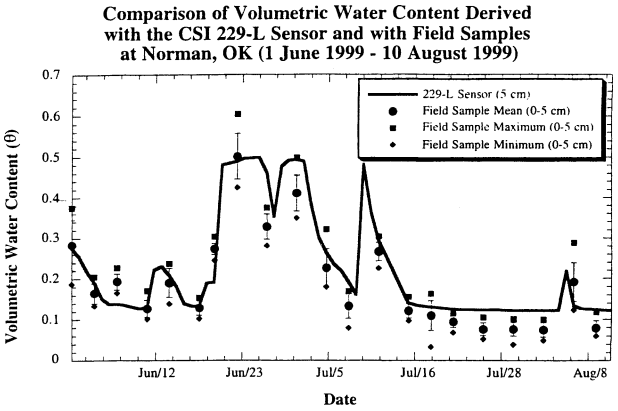

FIG. 3. Time series of 229-L volumetric water content at NORM, overlaid with field gravimetric sample mean, maximum, minimum, and standard deviation (represented by vertical error bars). Approximately 2272 discrete samples were analyzed for this figure [from Basara (2001), figure used with permission from Jeffrey Basara].

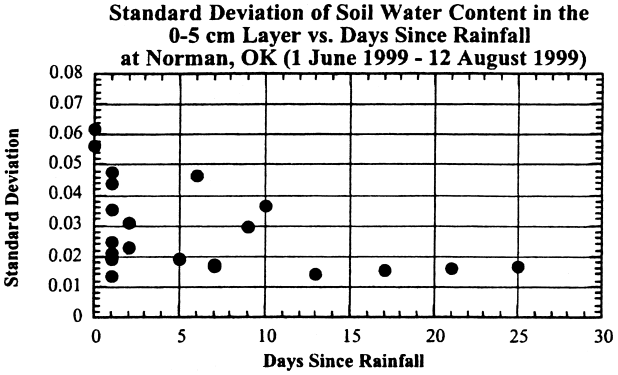

FIG. 4. Standard deviation of gravimetric field samples taken at NORM for the data presented in Fig. 3, as a function of days elapsed since last rainfall [from Basara (2001), figure used with permission from Jeffrey Basara].

short- and longwave) were measured. During both summers, the ground heat flux was measured with buried ground heat fluxes plates. During the summers of 1997 and 1998, additional instruments were installed at NORM to provide estimates of surface sensible and latent heat fluxes. During summer 1997 these instruments provided flux estimates via the Bowen ratio method (Bowen 1926), which assumes energy balance, and a bulk profile technique using similarity theory, following the relationships outlined by Halliwell and Rouse (1989). In July 1998, a field experiment was conducted to provide estimates of fluxes via the eddy covariance method (Arya 1988). During both field experiments, the flux estimates were compared against a variety of other independent observational techniques. Because of the inherent uncertainty regarding their use in validation of model data, we present some additional discussion of the surface energy flux and soil water observations at NORM and within the mesonet, particularly as it relates to instrument error and to what degree such data are spatially and temporally representative.

2) SOIL MOISTURE OBSERVATIONS

Soil moisture observations within the Oklahoma Mesonet are provided by the Campbell Scientific 229-L heat dissipation sensor. In order to obtain volumetric water content (the prognostic variable in the Eta Model), a soil-texture-dependent calibration is required. Preliminary calibrations, using soil texture data from mesonet sites, were provided using the method outlined by Arya and Paris (1981) and Schneider et al. (2003). Mesonet personnel continue to refine the calibration approach. Basara (2001) undertook an intensive field campaign during May–October 1999, wherein gravimetric samples were taken from 21 sites, geographically dispersed across the state of Oklahoma (in order to sample a variety of soil textures and soil moisture ranges). Gravimetric measurement, wherein a bulk sample of soil medium (including water) is weighed, oven dried, and then reweighed, provides the most straightforward method of measuring soil water content. Preliminary results from these data, which include over 4000 discrete samples, yield an average root-mean-square error for the corresponding 229-L estimates of 0.06 $m^3\ m^{-3}$ (J. B. Basara 2002, personal communication). Much of this field study was focused on the Norman site, where 2729 samples were taken from the landscape immediately adjacent to the 229-L sensor. Soil moisture data used in this study were collected from NORM with the same sensor as that used by the study of Basara (2001), and the same calibration technique used was applied to derive values of volumetric water content. Figure 3 shows the mean, maximum, minimum, and standard deviation of the samples as a function of sample day for the 0–5- and 5–10-cm gravimetric samples, with the corresponding time series for the 5-cm 229-L measurements overlaid. Figure 4 shows that the standard deviation of these measurements decreases with the time elapsed since rainfall. This decrease does not necessarily indicate increased accuracy of the 229-L sensors but does illustrate that the observed spatial variance (on the plot scale) is less at overall lower ranges. In fact, Schneider et al. (2003) show that the 229-L sensor may become less reliable at the lower ranges of soil water content. Nevertheless, at these observed ranges, the indicated error of the 229-L observations is within the range of model errors that will be presented in the results section.

Soil water and, to some extent, soil temperature point measurements are not as spatially representative as typical meteorological fields, because point observations can vary largely even on the plot scale, because of such factors as soil texture heterogeneity and preferred pathways for infiltration. This limitation renders comparison to model grid values of these variables a subject of considerable uncertainty. In producing gridded fields of soil moisture and temperature observations for comparison with model values, the three-pass Barnes ob-

jective analysis scheme utilized a radius of influence spanning the entire domain. Thus, the observational values were highly smoothed based on information from all other observations in the domain in the process of being interpolated to the model grid for comparison purposes. In this manner, we have attempted to remove some of the small-scale variability. According to Robock et al. (2003), large-scale smoothing and averaging of the Oklahoma Mesonet soil moisture data can be used to validate models with some reliability, because of the larger scale of soil moisture variation arising from the forcing of the land surface by the atmosphere at these scales, specifically as it relates to synoptic and mesoscale variation of precipitation. Given the plot-scale accuracy of this data, coupled with the interpolation and smoothing of the domain-wide observations, the authors believe that these data can be used in a meaningful manner for interpreting the performance of the Eta Model, particularly at NORM. Nevertheless, we wish to caution the reader to exercise care in the interpretation of the performance of the model vis-à-vis comparison with observed soil water data.

3) Surface flux estimates

As is the case with point-specific soil moisture data, great caution must be taken when drawing conclusions about model performance when comparing model grid values (which are representative of grid-box average conditions) to point-specific measures of surface fluxes. While the radiative components of the surface energy budget do vary somewhat smoothly in space and time under cloud-free conditions (e.g., downward solar radiation follows a sinusoidal diurnal curve that varies smoothly with latitude and longitude), the turbulent fluxes of sensible and latent heat can vary greatly over short distances, and on short timescales because of, among other factors, varying land surface properties. It should also be emphasized that direct measurements of surface energy and water fluxes do not exist; indeed, these quantities are merely estimates, which are ascertained using a variety of different instrument platforms and theoretical foundations. As such, the error in these estimates is an amalgam of the error inherent in the individual instrument platforms and assumptions of the theoretical underpinning.

In order to provide the reader with some measure of the reliability of the monthly average time series of estimates of these quantities, data from two different methods and/or instrument platforms that were periodically available at NORM during special field campaigns are provided. Unfortunately, data of this type spanning the July 1998 period were not available for this study. However, an eddy covariance system provided by the National Center for Atmospheric Research was collocated with the eddy covariance system that was located at NORM during part of this time for an intensive observing period as part of the Oklahoma Atmospheric Surface Layer Instrumentation System (OASIS; Brotzge and Weber 2002). For the July 1997 period of the study, data are available using two completely independent instrument platforms and estimation methodologies. In this instance, the Bowen ratio method and the bulk profile technique based on similarity theory were employed (Marshall et al. 1998). Figure 5 shows that differences between the bulk and Bowen ratio estimates of latent and sensible heat flux during July 1997 were as much as 50 W m^{-2}. The data from the 1998 OASIS project show maximum differences between the two eddy covariance systems of similar magnitude (Fig. 6). Table 1 provides a summary of the 24-h mean statistics for the days of data used to compile the monthly mean diurnal time series of observational differences presented in Figs. 5 and 6. In the next section, it will be shown that the model errors are typically less than the differences between the two different observational estimates, especially during the highly emphasized midday time range. Nevertheless, the observational differences can be close to the model error. Once again, caution must be emphasized with regard to drawing conclusions about model performance.

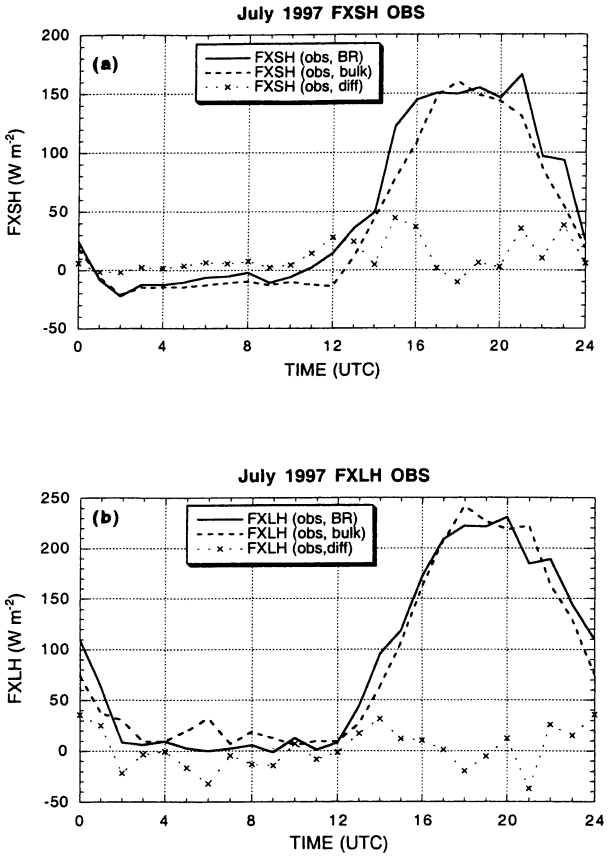

FIG. 5. Monthly mean diurnal time series of (a) FXSH and (b) FXLH for Jul 1997, for both the Bowen ratio (BR) and bulk profile (bulk) estimation methods, and the time series of the observational difference (diff).

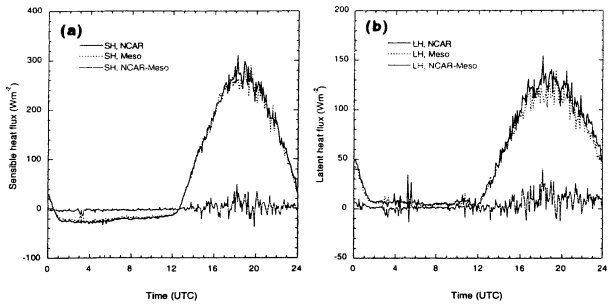

FIG. 6. Mean diurnal time series of (a) FXSH and (b) FXLH at NORM for the period 15 Jul–5 Aug 1998 (and the observational difference) provided by both the mesonet (Meso) eddy covariance system and NCAR eddy covariance systems [figure from Brotzge (2000), used with permission from Jerald Brotzge].

In addition to the error inherent in these point-specific measurements, there is also the question of what spatial area they represent, and how that impacts comparison with model gridpoint values. Mesonet personnel have completed only preliminary studies addressing this question, using limited field campaign data. We provide limited information based on these in-house studies, which suggest as distance approaches 100 km, the correlation coefficient for a subset of surface energy fluxes decreases to 0.1 (Fig. 7). These data are based on a field campaign during summer 1999, when sensible heat flux was measured via the profile technique at nine different sites spanning the network (Brotzge 2000).

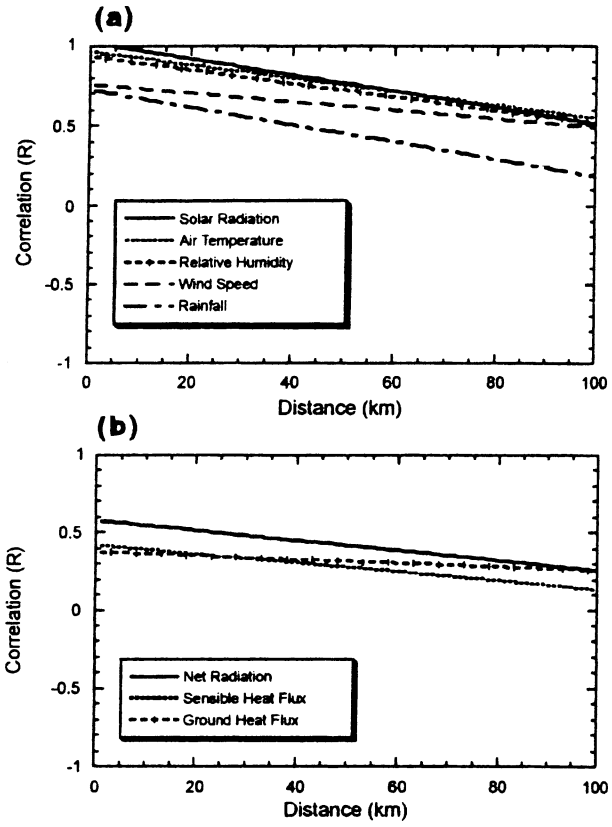

FIG. 7. Correlation coefficient as a function of distance for (a) selected meteorological parameters and (b) surface energy balance components. These data were produced using observation estimates from various field campaigns within the mesonet during 1999 [figure from Brotzge (2000), used with permission from Jerald Brotzge].

4. Summer 1997: Results and discussion

a. Surface fluxes and subsurface fields

During July 1997 the Eta Model top-layer soil moisture exhibited a pronounced positive bias over virtually the entire mesonet domain (Fig. 8). In some areas, the magnitude of the bias is a significant portion of the range of volumetric soil moisture contents observed in nature. The authors believe much of this error is the product of initialization from GDAS soil moisture. A high precipitation bias existed in the GDAS during the warm season time of this study, which may have contributed to a moist bias in its own internal soil moisture. Furthermore, during 1997, the GDAS employed a minimum-allowed value of 0.23 $m^3\ m^{-3}$, far higher than the value of 0.14 $m^3\ m^{-3}$ that is used in the EDAS for the predominant model soil type over Oklahoma (silty clay loam). The value assigned in GDAS was tuned to its own internal parameterizations, but it is inconsistent

TABLE 1. Standard deviation (std dev) mean, maximum (max), and minimum (min), for the difference of the monthly mean flux estimates for the periods Jul 1997 (''97'') and 15 Jul–5 Aug 1998 (''98''). For Jul 1997, differences are computed using Bowen ratio minus bulk profile data (for both FXSH and FXLH). For the 1998 period, differences are taken as NCAR minus Mesonet eddy covariance estimates. All units in W m^{-2}.

	FXSH 97	FXSH 98	FXLH 97	FXLH 98
Std dev	14.56	41.3	20.24	27.3
Mean	11.35	−1.26	2.1	5.2
Max	44.47	49	35.8	41.1
Min	−10.35	−18	−35.2	−12.5

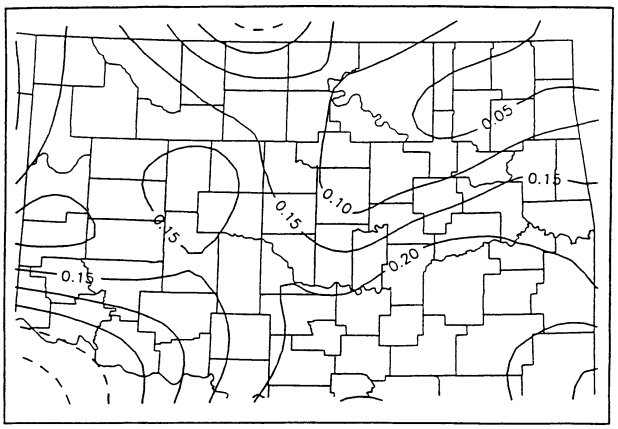

FIG. 8. Monthly mean of the daily bias in Eta Model soil moisture at 5 cm (SOIM) for Jul 1997 across the OK Mesonet domain. Solid (dashed) contours represent positive (negative) values.

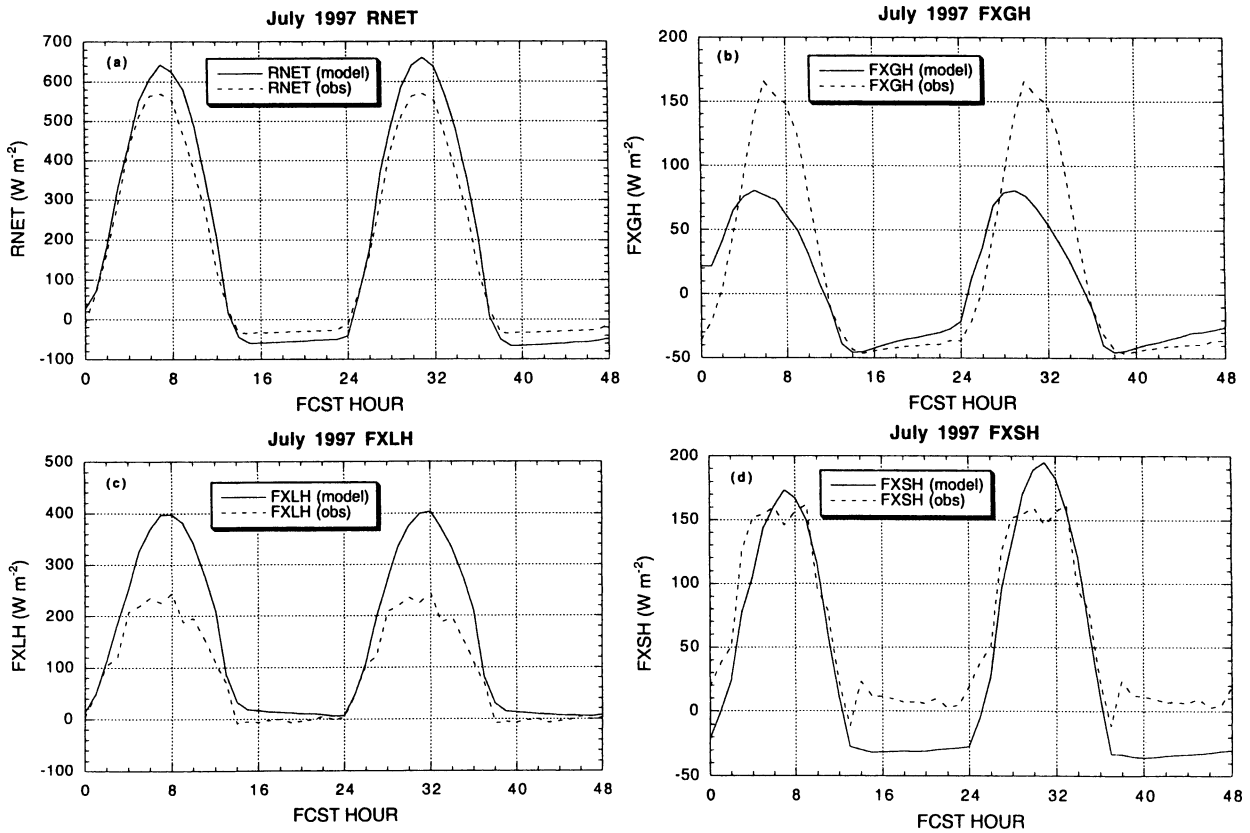

FIG. 9. Monthly mean diurnal cycle of the model and observed components of the surface energy budget at NORM for Jul 1997: (a) RNET, (b) FXGH, (c) FXLH, and (d) FXSH. Forecast hour (FCST HOUR) 0 corresponds to 1200 UTC on day 1 of the 48-h model forecast.

with the lower EDAS value, which is more typical of minimum values observed in nature. Thus, the soil moisture in the Eta Model was erroneously large not only because of faulty physics, but because the lower threshold imposed upon its initial value by the GDAS at the beginning of each 12-h data assimilation cycle was too high.

During the warm season of 1996, EMC personnel attempted to remedy this problem by applying an empirical reduction to the initial value of soil moisture as taken from the GDAS at the beginning of each 12-h EDAS cycle. However, internal verification procedures suggested that the reduction was too aggressive, resulting in an overly reduced surface latent heat flux and an attendant warm, dry bias in the PBL. The empirical reduction was removed prior to the 1997 warm season, and the initialization problem persisted until the implementation of continuous self-cycling in EDAS. It is important to emphasize that this issue represents a source of error for the land surface scheme that is not directly related to any inadequacy in the physics but is rather an initialization issue. Nevertheless, physical interpretation of the results of this study must account for it.

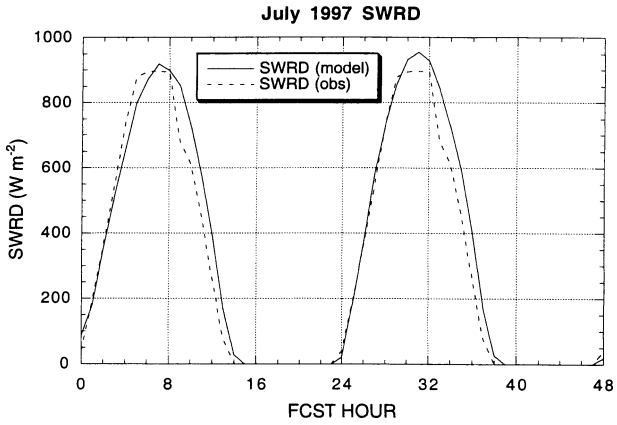

FIG. 10. Same as in Fig. 9 but for SWRD.

Not only do the initial conditions of land surface state variables present a source of error in the performance of the scheme, but so does the coupled model atmospheric forcing. The net radiation at the surface provides the source of energy for the surface turbulent and ground heat fluxes, and its accuracy is critical in determining their magnitudes. The monthly mean diurnal time series of net radiation at NORM for July 1997 (Fig. 9a) reveals a substantial positive bias in the model values—on the order of 75 W m^{-2} at midday. Much of this bias appears to be the result of an overestimate of downward shortwave radiation, which is also positively biased by 50–

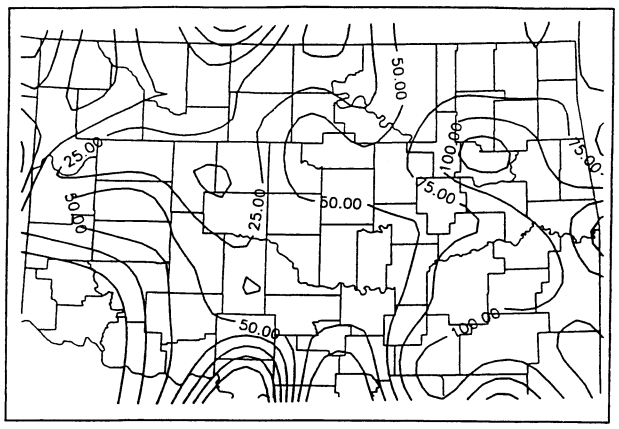

FIG. 11. Monthly mean of the midday (1800 UTC) bias in Eta Model SWRD for Jul 1997 across the OK Mesonet domain. Solid (dashed) contours represent positive (negative) values.

75 W m^{-2} at midday (Fig. 10). The monthly mean bias at midday across the mesonet domain shows a great deal of spatial variability (Fig. 11) and is generally higher than the midday bias in the diurnal time series at NORM. Recall, however, that cloudy days have been excluded from the composite time series. Thus, the spatial variability in Fig. 11 is a partial result of differences between model and observed cloudiness. Many other forecast models also exhibit a high bias in incoming solar radiation (Betts et al. 1997). In the Eta Model radiation treatment, absorption and attenuation of solar radiation by ozone and aerosols may be underestimated. Additionally, the effect of clouds (particularly warm season low-level cumulus clouds) on the reflection and absorption of incoming solar radiation is a difficult problem that is not well represented.

The monthly mean diurnal time series of ground heat flux (Fig. 9b) shows that the model values are overestimated in the morning, peak too early, and then become underestimated by 100 W m^{-2} at midday. Furthermore, the model time series is phase shifted by about -2 h from the observations. The large negative bias that dominates the majority of the daylight hours may be related to the empirical thermal conductivity (K_t) function. Peters-Lidard et al. (1998) have demonstrated that the function employed in the Eta Model (McCumber and Pielke 1981) is likely too nonlinear with respect to soil moisture content. In relatively dry soils, K_t, and hence ground heat flux, will be underestimated. Conversely, in moist soils, K_t is overestimated. Even though soil moisture is overestimated at NORM, K_t is still likely too small. This issue will be explored in detail in section 6.

The underestimate of ground heat flux during daylight hours should result in a cool bias in the 5-cm soil temperature if it were the only error-causing factor. Conversely, the slight overestimate during the nighttime hours should result in a warm bias. Monthly mean maps of 5-cm soil temperature (TSO5) bias (Fig. 12) show that, in general, at forecast hours 12 and 36 (late afternoon), there is a warm bias, with a cool bias developing by hours 24 and 48 (early morning). These results suggest that the diurnal cycle of 5-cm soil temperature is overamplified, which is physically inconsistent with the behavior of the model ground heat flux.

Many factors could be responsible for this inconsistency. First, the soil temperature is also a product of the specified soil heat capacity. If the soil heat capacity is underestimated, the temperature tendency could be too large despite the amount of ground heat flux. However, given that the soil moisture has a large positive bias, and the fact that the heat capacity is a very strong function of soil moisture content (more so than texture or any other variable), it is unlikely that the heat capacity has been underestimated. A second possible reason may be related to the fact that the soil temperature in a given layer is actually a product of the flux divergence in that layer. If the flux from layer 1 to layer 2 was more negatively biased than the surface ground heat flux during the daylight hours, too much energy would be stored in the first layer, possibly resulting in a warm bias. As with layer 1, it is likely that the thermal conductivity for layer 2 (and hence heat flux downward through the second layer) is also too small. Furthermore, the constant lower boundary condition for soil temperature could result in a misdiagnosed second-layer flux because of both its specified magnitude and the depth at which it is applied (3 m). In fact, observational evidence suggests that the annual cycle of the soil thermal wave may penetrate to depths of 10 m at some locations (Oke 1978). Unfortunately, the results presented here cannot include comparisons of model versus observed ground heat flux into the second soil layer, because model output of this variable was not archived by NCEP.

Because the land surface scheme adheres to surface energy balance constraints, the overestimate of net radiation, combined with the daytime underestimate of ground heat flux, result in too much available energy for the daytime turbulent fluxes. This excess energy must be partitioned between sensible and latent heat flux. In light of the very high bias in 5-cm soil moisture, it is not surprising that much of this excess is realized as excessive latent heat flux (Fig. 9c), which is nearly twice the observed at midday. However, the monthly mean diurnal cycle of sensible heat flux is fairly close to the observed (Fig. 9d). If the available energy (RNET $-$ FXGH) partitioning was correct, a positive bias in sensible heat flux should have been reflected in concomitant negative bias of similar magnitude in sensible heat flux. However, almost all of the excess is realized as latent heat flux.

b. PBL diurnal cycle

Given the large overestimate of daytime latent heat flux, it is not surprising that the monthly averaged diurnal time series of 2-m specific humidity (SPFH) exhibits a pronounced daytime moist bias (Fig. 13a). In-

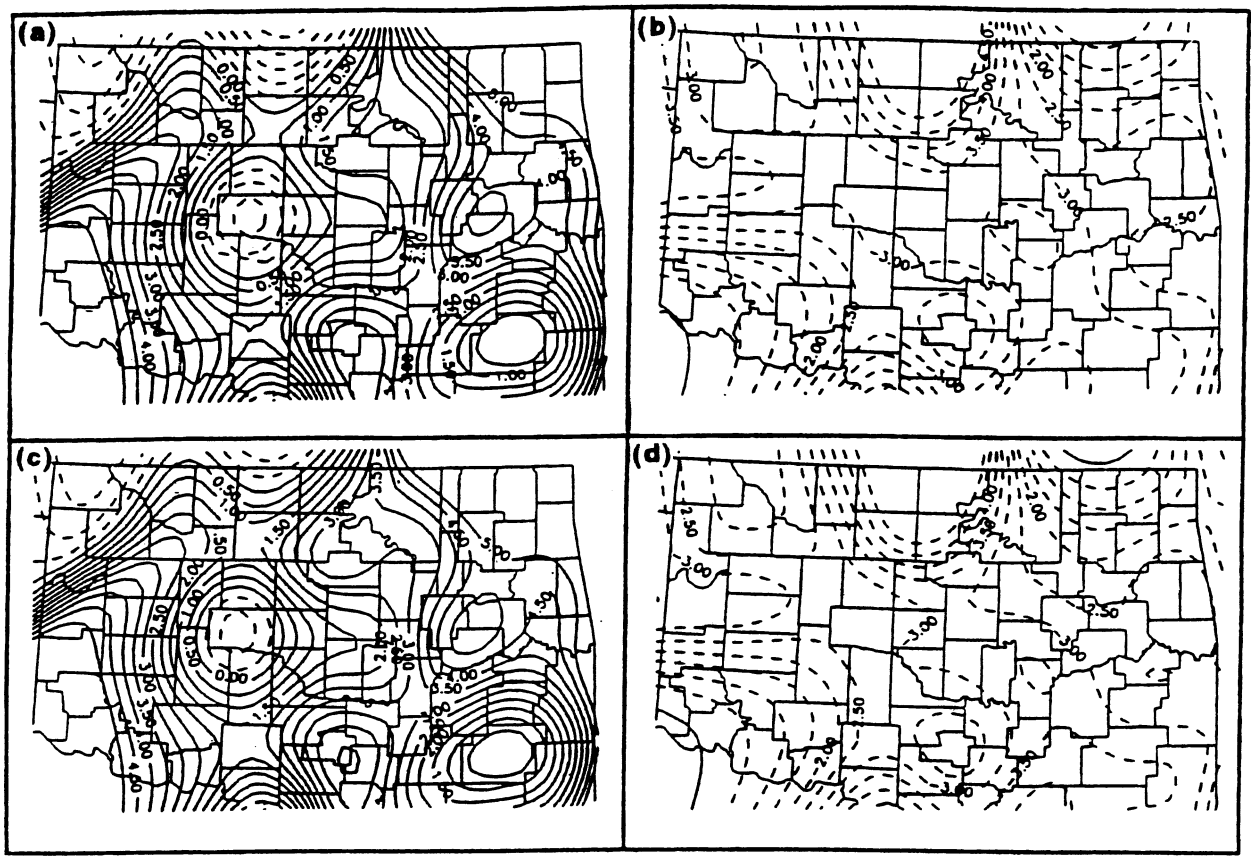

FIG. 12. Monthly mean diurnal cycle of bias in Eta Model TS05 at forecast hours (a) 12, (b) 24, (c) 36, and (d) 48. Solid (dashed) contours represent positive (negative) values.

deed, the model land surface is supplying the PBL with nearly twice the observed evaporation. The monthly averaged diurnal time series of 2-m air temperature (TAIR) exhibits a marked cool bias (Fig. 13b). This cool bias is not consistent with the error in the simulated sensible heat flux, which was very close to the observed composite time series.

Many physical processes are responsible for the diurnal evolution of near-surface thermodynamic quantities, and surface fluxes are only one contributor. If the PBL is treated as a slab model, and sources/sinks (such as direct radiative heating of PBL aerosols) are neglected, a scalar quantity "c" will evolve diurnally according to

$$\frac{\partial c}{\partial t} = -\mathbf{V}_H \cdot \boldsymbol{\nabla}_C + \overline{w'c'}|_B - \overline{w'c'}|_T, \qquad (3)$$

where $\mathbf{V}_H$ is the horizontal velocity, and w' and c' are the temporal perturbations of vertical velocity (w) and c, determined by Reynolds' averaging. The three terms on the right-hand side of (3) represent advection of c, the flux of c from the surface, and downward entrainment of c at the top of the PBL, respectively. Over long averaging periods with many samples, advective biases should be insignificant. The assumption is especially valid during midsummer synoptically quiescent periods when advection is minimal. However, entrainment can never be ignored when considering the diurnal evolution of the PBL. Comparison of model rawinsonde profiles with observations at NORM during July 1997 shows that the late afternoon (0000 UTC) well-mixed PBL was often too shallow. A classic example is presented in Fig. 14. In this case (24 July 1997), the PBL was too shallow by about 50 mb (as indicated by the height of the base of the thermal inversion at the top of the PBL), and too cool throughout its entire depth, despite near-observed sensible heat flux (Fig. 15a). The authors believe that, given the absence of large-scale dynamical forcing, this signature suggests a possible underestimate of downward entrainment at the top of the PBL.

Aside from demonstrating the general daytime moist bias due to the high latent heat flux, the time series of specific humidity for this case (Fig. 16) reveals some important behavior in the diurnal cycle of boundary layer moisture, which also suggests the entrainment process is not sufficiently represented. Shortly after initialization, a marked upward spike in model SPFH occurs. This spike, not as abrupt in the observations, suggests that the model PBL is not growing rapidly enough. By hour 4, model latent heat flux is already 150% of the observed (Fig. 15b). The net effect of these two

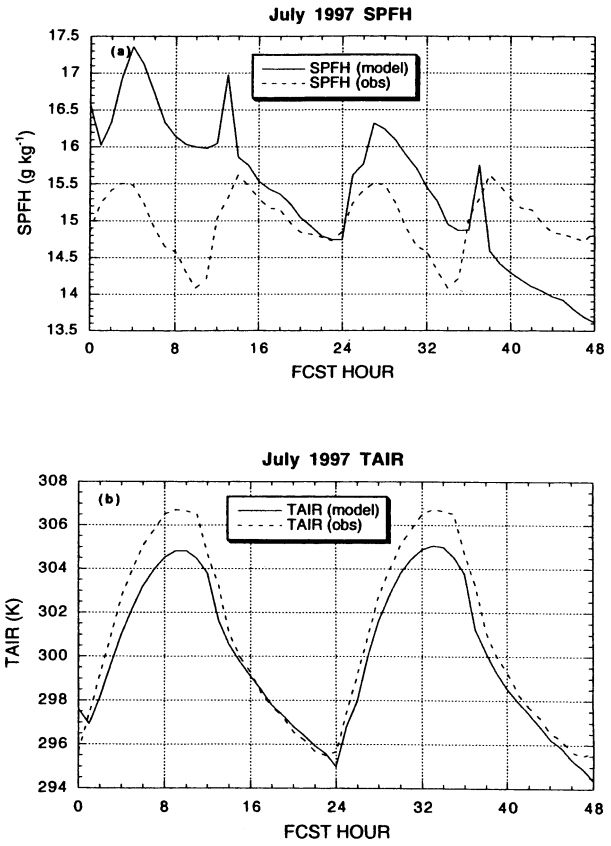

FIG. 13. Same as in Fig. 9 but for (a) SPFH and (b) TAIR.

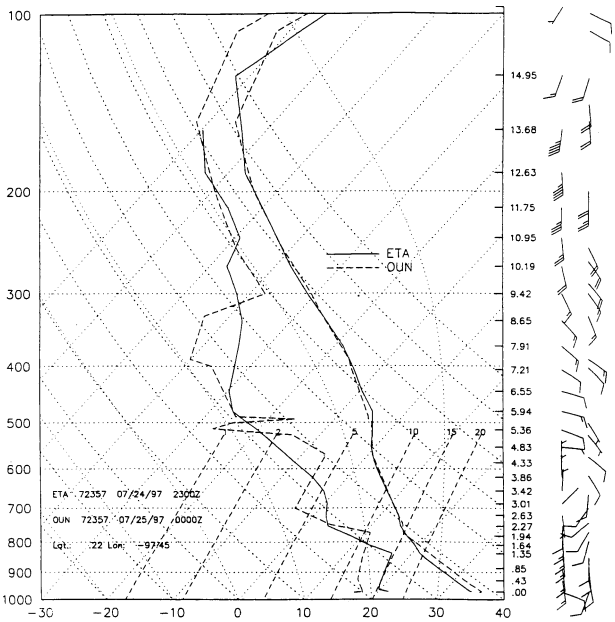

FIG. 14. Eta Model (ETA, solid curves) and observed (OUN, dashed curves) rawinsonde profiles (Skew*T*–log*p*) diagrams at Norman, OK, valid 0000 UTC 25 July 1997. The two leftmost (rightmost) curves are the dewpoint (temperature) profiles. Note that the Eta Model data valid at 2300 UTC 24 Jul are used in lieu of those for 0000 UTC 24 Jul, because this time corresponds more closely to the actual launch time of the OUN rawinsonde instrument.

factors is the evaporation of too much moisture into a PBL that is deepening too slowly, resulting in the exaggerated increase in PBL moisture shortly after sunrise. Shortly after the early morning maximum, specific humidity begins to decrease in both the model and the observations, as the entrainment at the top of the PBL serves to mix out the moisture. However, the observations show a sudden late morning decrease that is not adequately represented by the model. Rapid drying of PBL moisture during the late morning hours is typical during summer over the Great Plains, when strong mixing occurs in the PBL. Typically, a slight increase in PBL moisture occurs after sunrise in response to the onset of evapotranspiration. When the PBL deepens to the level of the preexisting residual layer by the late morning hours, rapid mixing and drying occur. The model time series of specific humidity reflects the overestimated evaporation after sunrise (particularly on day 1) and the possibility of underestimated PBL top entrainment. Similar behavior occurs on day 2, when the disparity between model and observed behavior in the rapid late morning decrease in specific humidity is even greater than on day 1.

Comparison of the composite time series of sensible heat flux and 2-m air temperature between May and July also supports the possibility of a systematic underestimate of entrainment. During May, NORM was affected twice by isolated convective rainfall that did not occur in the model, resulting in an unusual situation in which top-layer soil moisture was actually too dry during portions of the month (Fig. 17), despite erroneous initial conditions from GDAS. During the middle portion of the month, soil moisture was characteristically too large. However, many of those days were excluded from the composite time series of PBL fields due to cloudiness. Thus, the composite time series of sensible heat flux for May exhibits a substantial positive bias (Fig. 18), because it reflects primarily those days during which model soil moisture was too dry. Furthermore, the 2-m air temperature composite time series for those same days (Fig. 19) has no cool bias as in July. The May and July scenarios are physically consistent if a systematic underestimate of entrainment existed during both months. During May, the overestimated sensible heat flux may have acted to compensate for the lack of warm entrainment, thereby preventing a cool bias. When the monthly composite sensible heat flux was near the observed in July, this compensation was not present and the characteristic cool bias appeared.

It cannot be concluded from this analysis alone that this problem is associated with the PBL turbulence closure scheme, or if other factors are partially responsible. For example, the shallow convection parameterization, designed to account for the grid-scale effects of shallow, nonprecipitating convection in the lower to middle lev-

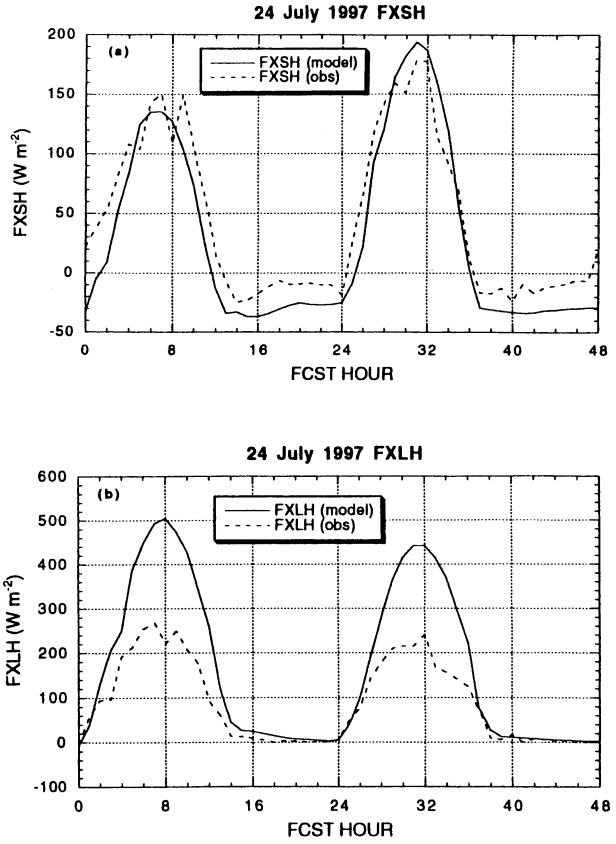

FIG. 15. Time series of the model and corresponding observed (a) FXSH and (b) FXLH for the model cycle beginning 1200 UTC 24 Jul 1997.

els of the troposphere (Betts 1974; Betts and Miller 1986; Janjić 1994), also could be a culprit. In fact, internal evaluation at EMC suggests that shallow convection may be too vigorous in certain environments, leading to overly strong midlevel subsidence and suppression of PBL growth. Regardless, the net effect appears to suppress the downward entrainment of relatively warmer, drier air into the convective PBL.

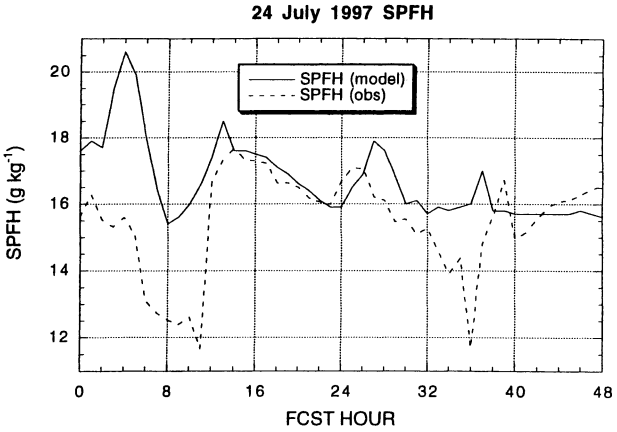

FIG. 16. Same as in Fig. 15 but for SPFH.

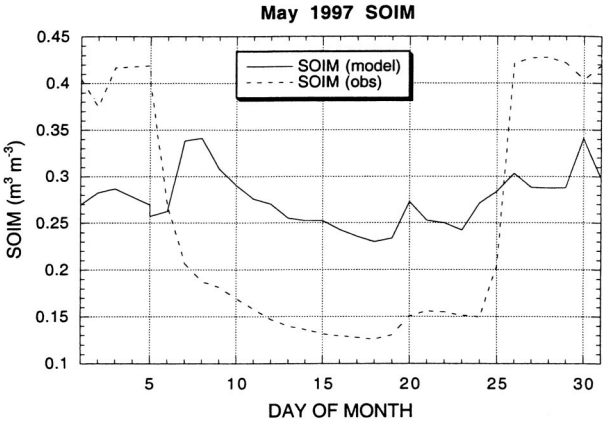

FIG. 17. Time series of model and observed 5-cm soil moisture (SOIN) at NORM for May 1997. Values are daily averages of hourly observations and model data.

The monthly composite biases of 2-m specific humidity and temperature at midday (1800 UTC) across the mesonet (Fig. 20) indicate very sharp gradients over the central part of the domain, which separate a cool/moist bias over western Oklahoma from a warm/dry bias in the east. Comparison of these fields with the model green vegetation fraction (σ_f) for July over Oklahoma (Fig. 21) reveals a striking spatial correlation between the sharp west–east gradient in greenness and the sharp west–east transition from the cool/moist bias to the warm/dry bias. The relationship between the spatial pattern of these biases and the distribution of σ_f suggests that over areas of relatively lower (higher) greenness, too much (little) latent heat flux is realized, despite overestimated soil moisture at all locations.

The cool/moist bias in the western part of the domain is consistent with the behavior of the model time series of surface fluxes and 2-m thermodynamic quantities at NORM. However, over eastern areas of the mesonet domain (east of NORM), the total evapotranspiration is more heavily dominated by canopy transpiration processes. As σ_f decreases westward, bare soil evaporation

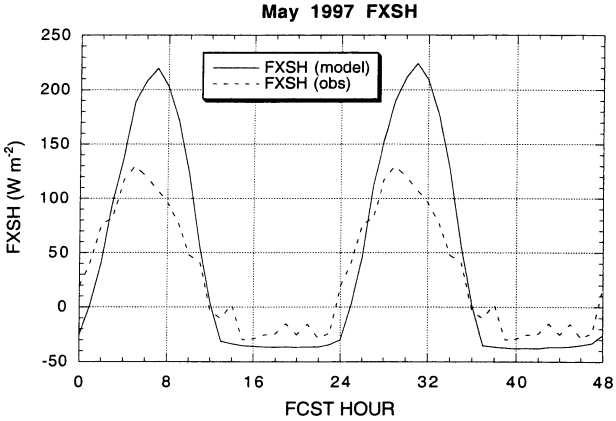

FIG. 18. Same as in Fig. 9 but for May 1997 FXSH.

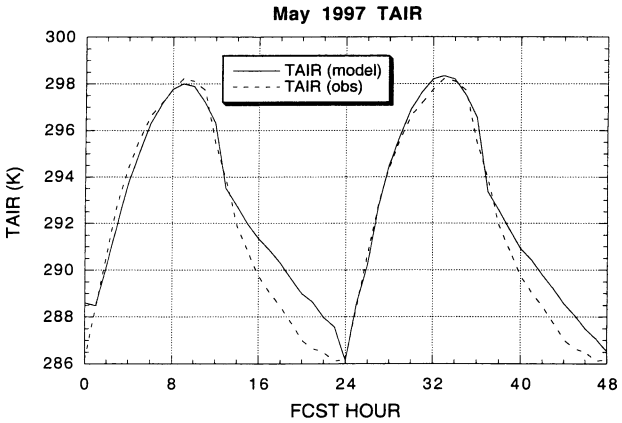

FIG. 19. Same as in Fig. 18 but for TAIR.

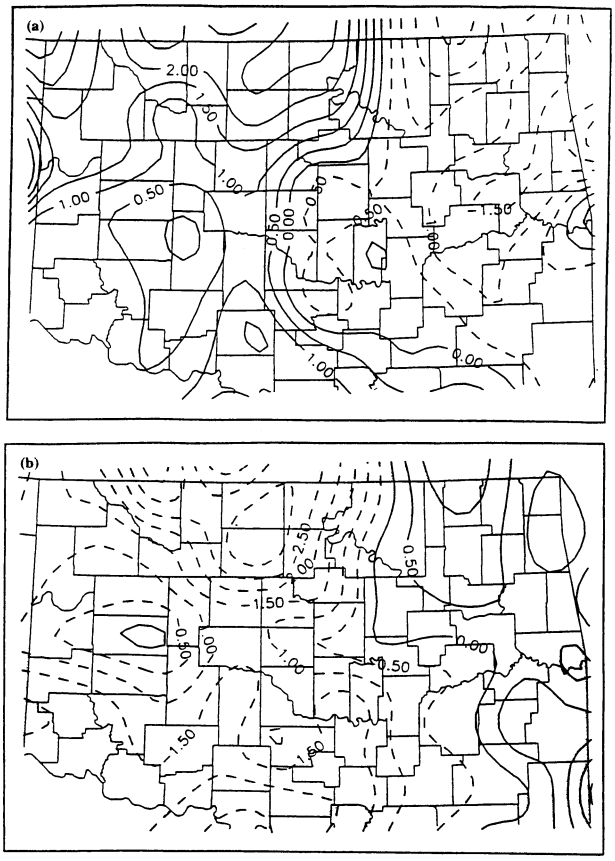

FIG. 20. Monthly mean of the midday (1800 UTC) bias in Eta Model (a) SPFH and (b) TAIR for Jul 1997 across the OK Mesonet domain. Solid (dashed) contours represent positive (negative) values.

becomes dominant [in accordance with Eq. (1)]. The bias patterns suggest that the land surface scheme is overestimating the canopy resistance, resulting in a warm/dry bias over areas where the canopy transpiration is the larger contributor to the total latent heat flux. Conversely, bare soil resistance is possibly underestimated, resulting in a cool/moist bias over areas where the bare soil evaporation is the larger contributor to the total latent heat flux.

The location of the greatest cool/moist bias is coincident with the distinct minimum in the greenness fraction over north-central Oklahoma. This area of the state is the heart of the winter wheat production region of the Great Plains. By July, senescence and harvest have occurred, leaving bare soil that dries rapidly. Climatological records indicate that shelter-level temperatures over this region are distinctly higher than surrouding areas during July (Johnson and Duchon 1995; Markowski and Stensrud 1998). The Eta Model land surface parameterization adequately incorporates the local vegetation phenology and contains the resolution and physics to capture this signature. However, the model signature is opposite to the observed. Two reasons are probably responsible for this behavior. First, the high top-layer soil moisture that results from the GDAS initialization is likely a major contributor to excess bare soil evaporation. Second, a different bare soil resistance formulation was employed in the Eta Model in February 1997. The old nonlinear function (not shown) was resulting in a rapid falloff in top-layer soil moisture, which in turn led to an underestimate of evaporation and an attendant warm/dry bias in the model PBL by day 2 of the 48-h forecast. To address this issue, a new linear stress function (designed to slow the evaporation at lower soil moisture values) was implemented. The resulting bare soil evaporation is very sensitive to the choice of values for the empirical constants that specify the available range of soil water (the air-dry value and the field capacity). Even if the soil moisture was more accurate, it is possible that the new linear function, designed to prevent the rapid falloff of bare soil evaporation, is contributing to its overestimation.

The canopy resistance physics are more complex than the bare soil physics, and the fact that top-layer soil moisture is too large will not necessarily result in too much transpiration. The effects of improper specification of various plant and aerodynamic resistance parameters can be just as important as the supplied soil moisture content in determining the resulting amount of transpiration. Furthermore, verification of deep-layer soil moisture (which is available to canopy transpiration via root uptake) was not possible in this study, and it is possible that the deep layer could actually be too dry. However, this is not likely given the initialization problems outlined above with the GDAS soil moisture, which was likely too high at lower levels because of the persistent high bias in GDAS precipitation.

5. Comparison of July 1998 to July 1997 surface fluxes

The findings presented in the previous section provide insight into the performance of the Eta Model land surface and PBL schemes that were operational during the

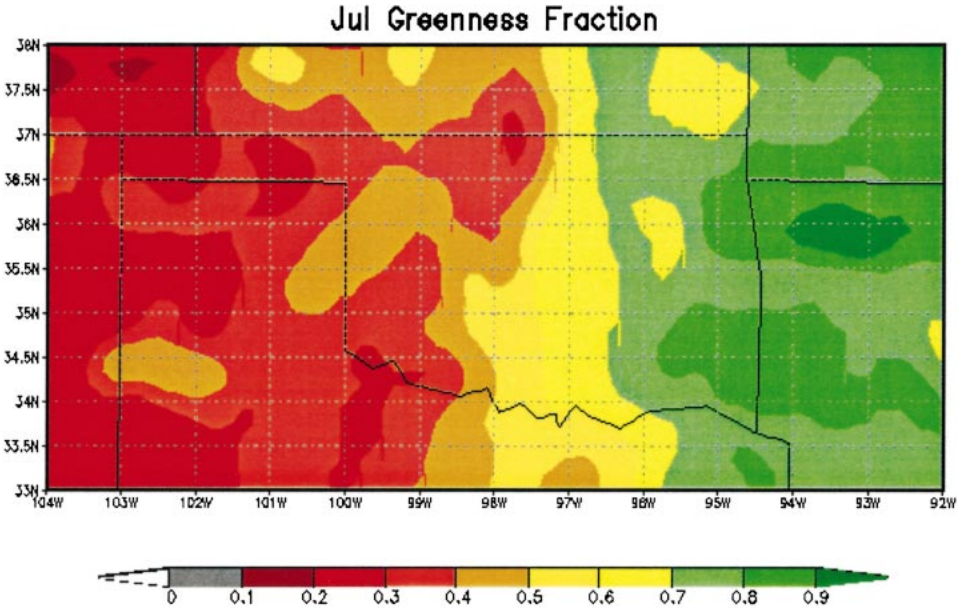

FIG. 21. Green vegetation fraction (σ_f) across OK for Jul. Note the sharp west–east gradient across the central part of the state.

warm season of 1997. Indeed, those results suggest that improvements were needed in several areas, including 1) the ground heat flux formulation, 2) canopy and/or aerodynamic resistance treatment (especially over heavily vegetated regions), 3) the bare soil evaporation stress function, and 4) the representation of entrainment processes at the top of the PBL. Nonetheless, the positive impacts of upgrades to the internal physics of the model cannot be realized fully if the initial conditions for the state variables are misdiagnosed in the operational environment. The initialization of soil moisture from the GDAS during summer 1997 was likely a major factor in degrading the operational performance of the land surface scheme, particularly over less vegetated regions. Furthermore, the interpretation of the results presented above is limited by this issue, because an objective assessment of the ability of the land surface physics to simulate time-dependent processes requires correct initial conditions for its state variables.

By July 1998, the land surface state variables (soil moisture and temperature) had been continuously cycling in the EDAS system for about 1 month. While this amount of time is not sufficient to allow model adjustment through the deeper layers, a sufficient amount of time had probably elapsed since the last initialization from the GDAS to allow EDAS top-layer soil moisture to reflect the stand-alone behavior of EDAS coupled model physics. The monthly mean bias in top-layer soil moisture over the mesonet domain during July 1998 (Fig. 22), compared with the same data for July 1997 (Fig. 8) reveals a significant decrease in the moist bias. Time series at NORM for both July periods (Fig.

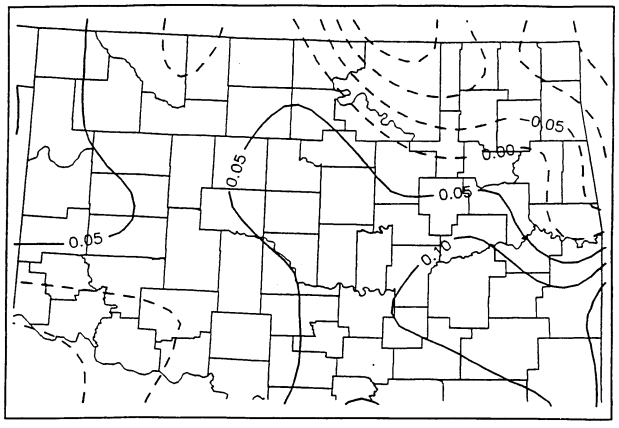

FIG. 22. Same as in Fig. 8 but for Jul 1998.

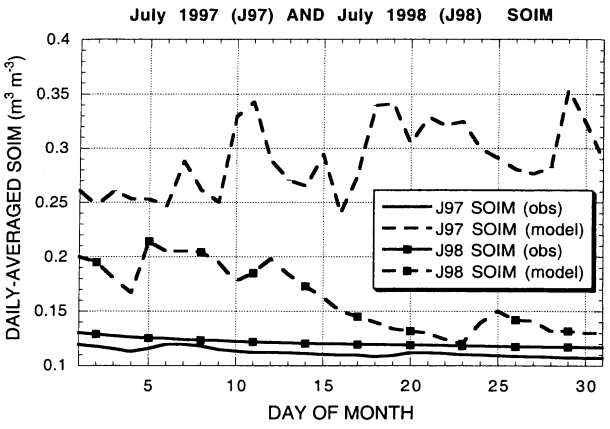

FIG. 23. Same as in Fig. 17 but for Jul 1997 and Jul 1998.

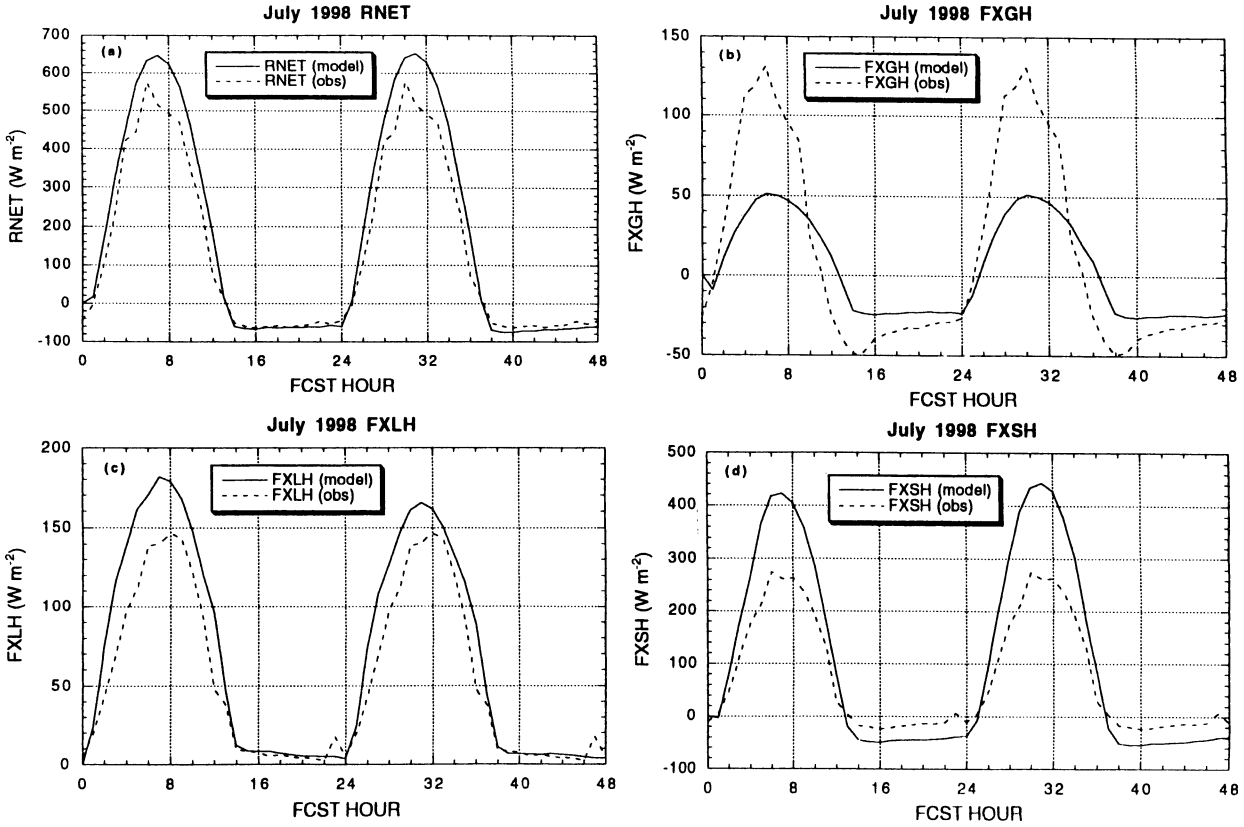

FIG. 24. Same as in Fig. 9 but for Jul 1998.

23) also illustrate the marked improvement in model performance. Both of the observational curves are near the minimum threshold much of the month, but the model curve for 1998 is much closer to the observed. Note also the general drying trend of the model during 1998, signaling that the soil moisture was cycling downward in the EDAS following the last erroneously high initialization from GDAS in early June. Evaluation of the surface fluxes during this period is of substantial interest, because their behavior should more accurately represent the behavior of the coupled model physics without contamination of the results by externally produced, erroneous initial conditions for soil moisture.

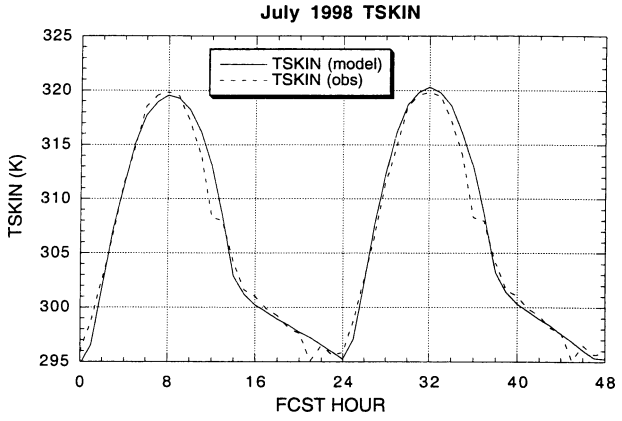

FIG. 25. Same as in Fig. 24 but for TSKIN.

The net radiation forcing continued to be too large during 1998 (Fig. 24a). Also, the behavior of ground heat flux during July 1998 (Fig. 24b) was similar to 1997, with a severe midday underestimate continuing. Again, this excess available energy must be distributed between sensible and latent heat flux. Because of the significant reduction of the positive soil moisture bias in 1998, it could be expected that more of this excess should be partitioned into sensible heat flux. In fact, the latent heat flux is much closer to the observed (Fig. 24c), and most of the excess is realized in overestimated sensible heat flux (Fig. 24d), despite the fact that soil moisture is not negatively biased. Given the availability of new data at NORM, the authors sought to explore this issue further. During July 1998, an additional sensor was installed at NORM to provide a radiometric measure of the skin temperature (T_{skin}). Examination of this variable (Fig. 25) reveals that the model time series matches the observations remarkably well. This result is inconsistent with the behavior of the model ground and sensible heat fluxes, because the skin temperature provides the upper-boundary condition for the calculation of the former and the lower-boundary condition for calculating the latter. Neither of these fluxes reflects

its accuracy, suggesting that other factors may be responsible for the underestimated ground heat flux and overestimated sensible heat flux. In the next section, we explore two other factors that are known to have a significant role in determining the values of skin temperature, ground heat flux, and sensible heat flux.

6. Sensitivity of the surface fluxes to the thermal roughness length and soil thermal conductivity

a. Background and method

Recall from section 2 that the sensible heat flux is calculated following the traditional bulk aerodynamic approach:

$$\mathrm{FXSH} = \rho c_p C_h |u_a| (T_{\mathrm{skin}} - T_a), \tag{4}$$

where ρ, c_p, C_h, $|u_a|$, and T_a are the air density, specific heat at constant pressure, surface exchange coefficient, wind speed at the first model level, and air temperature at the first model level, respectively. The surface exchange coefficient, C_h, provides the means of coupling the land surface to the PBL. Indeed, C_h is simply the mathematical inverse of the aerodynamic resistance. Assuming that the air temperature is relatively accurate, the primary parameters in determining the accuracy of sensible heat flux are the skin temperature and C_h. Thus, the overestimate of sensible heat flux during July 1998 may be related to the formulation of C_h, because simulated skin temperature was quite accurate (Fig. 25).

Quite often, the skin temperature is significantly too warm (cool) under thermodynamically unstable (stable) conditions when diagnosed from the energy balance equation (Sun and Mahrt 1995), leading to an over-(under-)estimate of the calculated sensible heat flux. In the Eta Model, this dilemma is addressed by introducing the concept of the thermal roughness length (Z_{0t}), which is used to determine the magnitude of C_h in such a way as to compensate for the use of skin temperature in the calculation of sensible heat flux. The formulation follows Zilitenkevich (1995) by defining Z_{0t} as a fraction of the momentum roughness length. In particular, the ratio of the two roughness lengths is expressed as a function of the turbulence of the flow:

$$\frac{Z_{0m}}{Z_{0t}} = \exp(kC\sqrt{\mathrm{Re}^*}). \tag{5}$$

The degree of turbulence is specified by the Reynolds number (not shown), where k is the von Kármán constant and C is a tunable factor. It is this latter parameter that Chen et al. (1997) demonstrated to have the most impact on the resulting magnitude of C_h and, hence, sensible heat flux. Their sensitivity studies demonstrated the impact of order-of-magnitude differences in C (ranging from 0.01 to 10), and resulted in the operational implementation of a value of 0.1. An increase (decrease) in the value of C leads to smaller (larger) C_h.

In addition to its use in calculating sensible heat flux, the skin temperature is also intimately related to ground heat flux. As discussed above, other factors that strongly influence the magnitude of the ground heat flux include the empirical specification of the soil thermal conductivity (K_t). Figure 26, the Eta Model formulation of K_t and an alternative one proposed by Peters-Lidard et al. (1998) for silty clay loam (the model soil type at NORM), highlights the large differences among empirical choices. Note that the Eta Model version is highly nonlinear with respect to soil moisture content, especially in the middle ranges. In particular, the magnitude is roughly one-half that of the alternative function at 50% saturation, which roughly corresponds to the soil moisture observed at NORM during July 1998.

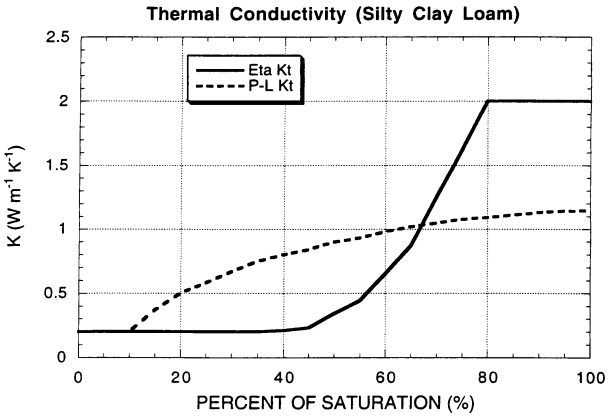

FIG. 26. Thermal conductivity (K_t) as a function of percent of soil saturation for the current operational Eta Model (Eta) and the alternative function (P-L) from Peters-Lidard et al. (1998).

Given the physical inconsistencies among the fluxes and the skin temperature errors during July 1998, we have undertaken three sensitivity tests to examine the impact of the value of C and the alternative K_t. The 1200 UTC model cycle from 18 July 1998 is used as the experimental control for these tests. This day was chosen because, much like the 24 July 1997 case study, conditions were synoptically quiescent with little cloud cover and strong PBL mixing. It is also highly representative of the monthly composite data. The first test (T1) employs the Peters-Lidard value for K_t that corresponds to the model soil moisture at NORM on 18 July. The second test (T2) examines the sensitivity of the surface fluxes to C within its operational order of magnitude, by assigning a value of 0.2. A higher (as opposed to lower) value is chosen to investigate the impact on reducing the overestimated sensible heat flux when using the default value of 0.1. The third test (T3) includes both T1 and T2. All three test integrations were performed using the same resolution and initial conditions as the control. Also, each integration began with a 12-h EDAS cycle, followed by the 48-h free-forecast results presented here.

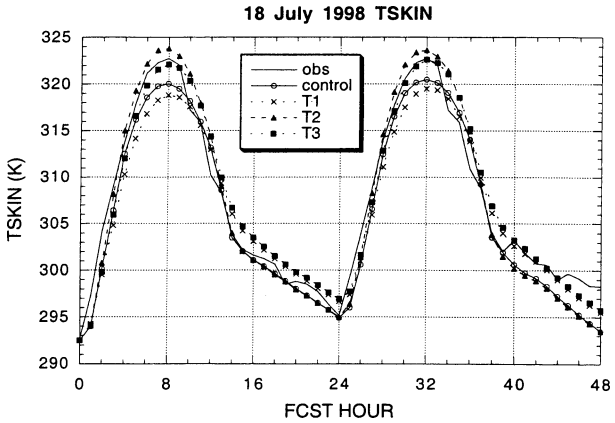

FIG. 27. Sensitivity tests for the dependence of T_{skin} on the soil thermal conductivity (test T1), the C parameter of the Zilitenkevich formulation (T2), and both (T3) for the model cycle beginning 1200 UTC 18 Jul 1997.

b. Results

As expected, the use of the alternative K_t function in T1 decreased the value of the daytime skin temperature (Fig. 27). For all three tests, the simulated value of RNET was not changed appreciably (Fig. 28a) and exhibited the typical midday high bias. The use of the Peters-Lidard function for K_t greatly improved the simulated ground heat flux (Fig. 28b). The control experiment was characterized by the typical severe negative bias, but the simulated value more than doubled with the use of the new K_t. The T1 value is much closer to the observations, with a midday negative bias of 20 W m^{-2}. Furthermore, the T1 time series is more in phase with the observed cycle than the control, and the distinct nighttime minimum at hours 14 and 38 is captured more precisely. The latent heat flux (Fig. 28c) is changed little from the control, because the evaporation physics are not as sensitive to the aerodynamic resistance (i.e., the C parameter) and skin temperature as the bulk aerodynamic formulation for sensible heat flux. Because of the positive soil moisture bias at NORM, it is reasonable that latent heat flux should be overestimated for all of the experiments.

Again, it is interesting to note that sensible heat flux is about 100 W m^{-2} too large at midday in the control case, despite the fact that the skin temperature is actually about 2.5 K too cool. This relationship attests to the fact that other factors are resulting in the inflated sensible heat flux. The decrease in skin temperature in T1 (about 1 K at midday) results because more energy is being removed from the surface via conduction into the soil. In turn, the lowered skin temperature results in somewhat less sensible heat flux (Fig. 28d). Increasing the value of C in the Zilitinkevich formulation from 0.1

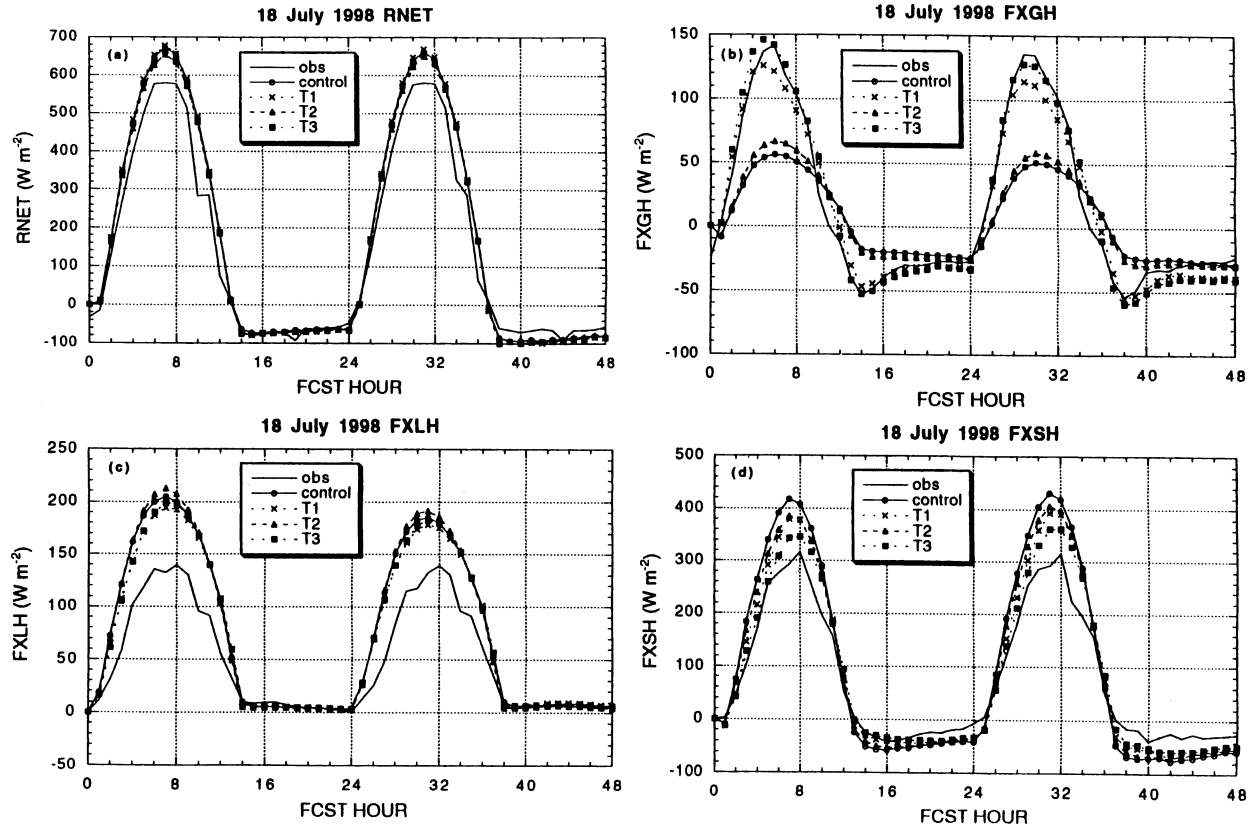

FIG. 28. Same as in Fig. 27 but for (a) RNET, (b) FXGH, (c) FXLH, and (d) FXSH.

to 0.2 (T2) also results in a lowered sensible heat flux. However, the magnitude of the reduction is nearly the same as the reduction afforded by only using the new K_t. Without the new K_t, however, the new C value (T2) results in a near 4 K increase in the midday skin temperature. Even in the face of this substantial difference in skin temperature, the ground heat flux in T2 is changed little from the control. These results support the previous study by Chen et al. (1997) that showed the skin temperature to be very sensitive to the choice of C. These results go one step further in demonstrating that this sensitivity is greater than the sensitivity of skin temperature to the thermal conductivity specification. Test T1 resulted in only a 1-K change in skin temperature, while T2 yielded a change of 4 K. Furthermore, T1 actually resulted in a cooler value than the control, which is already 2.5 K less than the observed at midday.

The third test (T3) reveals that when both of the changes above are combined, skin temperature, ground heat flux, and sensible heat flux are closer to their respective observed values than for either change alone. Based on this result, the authors believe that the lower value of C in the control is acting to compensate for the underestimated thermal conductivity in determining the simulated skin temperature. Because of balance requirements, the excess energy input from the too high net radiation must be removed from the surface via conduction into the soil or via convective transport into the atmosphere. In the control case, the underestimated soil conductivity appears to limit the conductive mechanism, while the lower value of C increases the magnitude of C_h (i.e., decreases the aerodynamic resistance), thereby allowing the heat to be removed from the surface via convective transport. This interaction also explains why the excess available energy for turbulent fluxes is being partitioned mostly into sensible heat flux in the control, despite a positive soil moisture bias. In other words, these results show that the values of skin temperature, ground heat flux, and sensible heat result from a delicate balance between the values of the empirical value chosen for C and the soil conductivity formulation. These parameters must be finely tuned to achieve the greatest accuracy in the surface fluxes, notwithstanding the accuracy of the model soil moisture.

7. Summary, conclusions, and future work

With the implementation of a land surface scheme in the Eta Model, more realistic simulation of the interaction between the surface of the earth and the atmosphere is possible, especially in representing the diurnal cycle of PBL growth and decay. These advancements notwithstanding, several key problems were found and addressed in this study, as summarized below:

- high initial soil moisture from GDAS, largely remedied by the implementation of continuous self-cycling of soil moisture in EDAS on 9 June 1998;
- overestimated downward shortwave radiation from possible underestimates of cloud cover, and lack of attenuation and absorption by aerosols and ozone;
- possible overly large canopy resistance, resulting in a near-surface warm/dry bias in heavily vegetated regions of the model domain;
- severe daytime underestimate of ground heat flux in drier soils; and
- possible underestimate of entrainment at the top of the PBL.

By July 1998, EDAS soil state variables were continuously self-cycling (i.e., the GDAS initialization error was removed), and the number of soil layers had increased from two to four. Verification of top-layer soil moisture showed that the positive bias had been substantially reduced when compared to July 1997. Thus, the performance of the surface fluxes was revisited and compared to the July 1997 performance. Unexpected and physically inconsistent behavior was noted among the surface fluxes and the simulated skin temperature, prompting the authors to undertake a series of sensitivity tests. These tests confirmed the earlier results of Chen et al. (1997) wherein the large sensitivity of the skin temperature to the ''C parameter'' was shown, but also demonstrated further that the skin temperature is much more sensitive to the C parameter than to the value of the soil thermal conductivity. Furthermore, the interaction of these parameters was shown to be very important in determining the partitioning of net radiation between conducted and convective forms of energy at the surface of the earth.

The findings presented in this paper are not intended to provide a universal blueprint for the performance of the Eta Model land surface parameterization at all locations and times. Indeed, upgrades to operational model physics are a continuous process in the operational environment, requiring continuing verification and sensitivity studies. Because of the inherent problems of verifying the model against observed estimates of surface fluxes and soil state variables, the interpretation of results such as those presented in this paper must be undertaken with the utmost caution. Nonetheless, these findings contributed scientific evidence in support of operational model upgrades.

To further address the issues outlined in this paper and other verification studies, NCEP has embarked on a collaborative effort to develop a North American land data assimilation system (NLDAS; Mitchell et al. 2003). In the NLDAS configuration, the land surface physics are integrated in an uncoupled mode, using observed rainfall and satellite-based downward shortwave radiation as forcing, rather than coupled model input of these quantities. In addition, complex frozen soil and snowpack physics are included in the NLDAS, as well as very high resolution soil and vegetation databases. Some of the improvements resulting from research and development of the NLDAS have already been imple-

mented in the operational Eta Model (Ek et al. 2003). When NLDAS becomes operational, the improved soil moisture and temperature from this system will supply initial conditions to NCEP operational forecast models. In turn, the improved soil states will result in better surface fluxes and improved forecasts of PBL structure.

Acknowledgments. Part of this research was supported by a graduate fellowship for the first author from the Cooperative Program for Operational Meteorology Education and Training (COMET). Portions of this research were completed while the first author was employed at the NOAA/NWS/NCEP/Environmental Modeling Center. The technical staff at the Oklahoma Mesonet provided invaluable assistance with the installation of additional observational platforms at the Norman Oklahoma Mesonet site. Dale Morris of the Oklahoma Climate Survey contributed his substantial technical expertise in the analysis of the resulting datasets. We thank Eric Rogers and Geoff Manikin of NCEP/EMC for their assistance in running the Eta Model. Three anonymous reviewers provided valuable comments that have resulted in a more solid manuscript, particularly as they relate to the use of surface flux and soil water data in the verification of models.

REFERENCES

Arya, L. M., and J. F. Paris, 1981: A physioempirical model to predict the soil moisture characteristic from particle-size distribution and bulk density data. *Soil Sci. Soc. Amer. J.,* **45,** 1023–1030.

Arya, S. P., 1988: *Introduction to Micrometeorology.* Academic Press, 307 pp.

Basara, J. B., 2001: The value of point-scale measurements of soil moisture in planetary boundary layer simulations. Ph.D. dissertation, University of Oklahoma, 225 pp. [Available from School of Meteorology, 100 E. Boyd, Suite 1310, Norman, OK 73019-1012.]

Betts, A. K., 1974: Reply to comment on the paper ''Non-precipitating cumulus convection and its parameterization.'' *Quart. J. Roy. Meteor. Soc.,* **100,** 464–471.

——, and M. T. Miller, 1986: A new convective adjustment scheme. Part I: Observational and theoretical basis. *Quart. J. Roy. Meteor. Soc.,* **112,** 677–691.

——, F. Chen, K. Mitchell, and Z. I. Janjić, 1997: Assessment of the land surface and boundary layer models in two operational versions of the NCEP Eta Model using FIFE data. *Mon. Wea. Rev.,* **125,** 2896–2916.

Black, T. L., 1994: The new NMC mesoscale Eta Model: Description and forecast examples. *Wea. Forecasting,* **9,** 265–278.

Bowen, I. S., 1926: The ratio of heat losses by conduction and by evaporation from any water surface. *Phys. Rev.,* **27,** 779–787.

Brock, F. V., K. C. Crawford, R. L. Elliott, G. W. Cuperus, S. J. Stadler, H. L. Johnson, and M. D. Eilts, 1995: The Oklahoma Mesonet: A technical overview. *J. Atmos. Oceanic. Technol.,* **12,** 5–19.

Brotzge J. A., 2000: Closure of the surface energy budget. Ph.D. dissertation, University of Oklahoma, 208 pp. [Available from School of Meteorology, 100 E. Boyd, Suite 1310, Norman, OK 73019-1012.]

——, and D. Weber, 2002: Land-surface validation using the Oklahoma Atmospheric Surface Layer Instrumentation System (OASIS) and Oklahoma Mesonet data: Preliminary results. *Meteor. Atmos. Phys.,* **80,** 189–206.

Chen, F., and Coauthors, 1996: Modeling of land surface evaporation by four schemes and comparison with FIFE observations. *J. Geophys. Res.,* **101,** 7251–7268.

——, Z. Janjić, and K. Mitchell, 1997: Impact of atmospheric surface-layer parameterization in the new land-surface scheme of the NCEP mesoscale Eta Model. *Bound.-Layer Meteor.,* **85,** 391–421.

Cosby, B. J., G. M. Hornberger, R. B. Clapp, and T. R. Ginn, 1984: A statistical exploration of the relationships of soil moisture characteristics to the physical properties of soils. *Water Resour. Res.,* **20,** 682–690.

Ek, M. B., K. E. Mitchell, Y. Lin, E. Rogers, P. Grunmann, V. Koren, G. Gayno, and J. D. Tarpley, 2003: Implementation of Noah land-surface model advances in the NCEP operational mesoscale Eta model. *J. Geophys. Res.,* in press.

Gutman, G., and A. Ignatov, 1998: The derivation of green vegetation fraction from NOAA/AVHRR for use in numerical weather prediction models. *Int. J. Remote Sens.,* **19,** 1533–1543.

Haliwell, D. H., and W. R. Rouse, 1989: A comparison of sensible and latent heat flux calculations using the Bowen Ratio and aerodynamic methods. *J. Atmos. Oceanic Technol.,* **6,** 563–574.

Hanks, R. J., and G. L. Ashcroft, 1986: *Applied Soil Physics.* Springer-Verlag, 159 pp.

Jacquemin, B., and J. Noilhan, 1990: Sensitivity study and validation of a land surface parameterization using the HAPEX-MOBILHY dataset. *Bound.-Layer Meteor.,* **52,** 93–134.

Janjić, Z. I., 1994: The step-mountain eta coordinate model: Further developments of the convection, viscous sublayer, and turbulence closure schemes. *Mon. Wea. Rev.,* **122,** 927–945.

Johnson, H. L., and C. E. Duchon, 1995: *Atlas of Oklahoma Climate.* University of Oklahoma Press, 118 pp.

Kanamitsu, M., and Coauthors, 1991: Recent changes implemented into the global forecast system at NMC. *Wea. Forecasting,* **6,** 425–435.

Kim, J., and S. B. Verma, 1990: Components of surface energy balance in a temperature grassland ecosystem. *Bound.-Layer Meteor.,* **51,** 401–417.

Łobocki, L., 1993: A procedure for the derivation of surface-layer bulk relationships from simplified second-order closure models. *J. Appl. Meteor.,* **32,** 126–138.

Mahrt, L., and K. Ek, 1984: The influence of atmospheric stability on potential evaporation. *J. Climate Appl. Meteor.,* **23,** 222–234.

——, and H.-L. Pan, 1984: A two-layer model of soil hydrology. *Bound.-Layer Meteor.,* **29,** 1–20.

Markowski, P. M., and D. J. Stensrud, 1998: Mean monthly diurnal cycles observed with PRESTORM surface data. *J. Climate,* **11,** 2995–3009.

Marshall, C. H., K. C. Crawford, and J. A. Brotzge, 1998: A comparison of the Bowen ratio and aerodynamic methods to Oklahoma Mesonet estimate of surface latent flux. Preprints, *10th Symp. on Meteorological Observations and Instrumentation,* Phoenix, AZ, Amer. Meteor. Soc., 323–328.

McCumber, M. C., and R. A. Pielke, 1981: Simulation of the effects of surface fluxes of heat and moisture in a mesoscale numerical model. *J. Geophys. Res.,* **86** (C10), 9929–9938.

Mellor, G. L., and T. Yamada, 1974: A hierarchy of turbulence closure models for planetary boundary layers. *J. Atmos. Sci.,* **31,** 1791–1806.

Mesinger, F., 1984: A blocking technique for representation of mountains in atmospheric models. *Riv. Meteor. Aeronaut.,* **44,** 195–202.

Mitchell, K. E., and Coauthors, 2003: The multi-institution North American Land Data Assimilation System (NLDAS): Utilizing multiple GCIP products and partners in a continental distributed hydrological modeling system. *J. Geophys. Res.,* in press.

Monin, A. S., and A. M. Obukhov, 1954: Basic laws of turbulent mixing in the atmosphere near the ground. *Tr. Akad. Nauk SSSR Geoph. Inst.,* **24,** 1963–1987.

Noilhan, J., and S. Planton, 1989: A simple parameterization of land

surface processes for meteorological models. *Mon. Wea. Rev.*, **117,** 536–549.

Oke, T. R., 1978: *Boundary Layer Climates.* Cambridge University Press, 435 pp.

Pan, H.-L., and L. Mahrt, 1987: Interaction between soil hydrology and boundary-layer development. *Bound.-Layer Meteor.*, **38,** 185–202.

Paulson, C. A., 1970: The mathematical representation of wind speed and temperature profiles in the unstable atmospheric surface layer. *J. Appl. Meteor.*, **9,** 857–861.

Peters-Lidard, C. D., E. Blackburn, X. Liang, and E. F. Wood, 1998: The effect of soil thermal conductivity parameterization on surface energy fluxes and temperatures. *J. Atmos. Sci.,* **55,** 1209–1224.

Pielke, R. A., G. A. Dalu, J. S. Snook, T. J. Lee, and T. G. F. Kittel, 1991: Nonlinear influence of mesoscale land use on weather and climate. *J. Climate*, **4,** 1053–1069.

Robock, A., and Coauthors, 2003: Validation of North American Land Data Assimilation Systems retrospective forcing over the southern Great Plains. *J. Geophys. Res.*, in press.

Rogers, E., T. L. Black, D. G. Deaven, G. J. DiMego, Q. Zhao, M. E. Baldwin, N. W. Junker, and Y. Lin, 1996: Changes to the operational early Eta analysis/forecast system at the National Centers for Environmental Prediction. *Wea. Forecasting,* **11,** 391–413.

Schaake, J. C., V. I. Koren, Q. Y. Duan, K. Mitchell, and F. Chen, 1996: Simple water balance model for estimating runoff at different spatial and temporal scales. *J. Geophys. Res.*, **101,** 7461–7475.

Schneider, J. M., D. K. Fisher, R. L. Elliott, G. O. Brown, and C. P. Bahrmann, 2003: Spotiotemporal variations in soil water: First results from the ARM SGP CART network. *J. Hydrometeor.*, **4,** 106–120.

Sorbjan, Z., 1989: *Structure of the Atmospheric Boundary Layer*. Prentice Hall, 317 pp.

Sun, J., and L. Mahrt, 1995: Determination of surface fluxes from the surface radiative temperature. *J. Atmos. Sci.,* **52,** 1096–1104.

Xue, Y., M. Fennessy, and P. Sellers, 1996: Impact of vegetation properties on U.S. summer weather prediction. *J. Geophys. Res.*, **101,** 7419–7430.

Zilitinkevich, S. S., 1995: Non-local turbulent transport: pollution dispersion aspects of coherent structure of convective flows. *Air Pollution Theory and Simulation,* Vol. 1, H. Power, N. Moussiopoulos, and C. A. Brebbia, Eds., *Air Pollution III*, Computational Mechanics Publications, 53–60.

Zobler, L., 1986: A world soil file for global climate modelling. NASA Tech. Memo. 87802, 33 pp. [Available from NASA Goddard Space Flight Center, Institute for Space Studies, 2800 Broadway, New York, NY 10025.]